RE-EVALUATION OF THE CIRCADIAN CLOCK MODEL IN MAMMALS

哺乳類の概日時計モデルの再検討に関する研究

APIRADA PADLOM

LABORATORY OF ANIMAL INTEGRATIVE PHYSIOLOGY

DEPARTMENT OF ANIMAL SCIENCES

GRADUATE SCHOOL OF BIOAGRICULTURAL SCIENCES

NAGOYA UNIVERSITY

2023

Acknowledgement

I would like to express my sincere gratitude and deepest appreciation to the following people who have contributed to the success of this dissertation:

To Associate Professor Dr. Taeko Ohkawa from the Graduate School of Bioagricultural Sciences, Nagoya University for her guidance and supervision of this research, for kindly teaching me many techniques which I have never experienced before, for her creative and interesting ideas, which constantly inspire me to be enthusiastic about science and teach me about logical reasoning and how to be a good scientist.

To Professor Dr. Takashi Yoshimura from the Graduate School of Bioagricultural Sciences, Nagoya University, for his generosity in providing me an opportunity to study at Nagoya University.

To Yuko Furukawa from the Institute of Transformative Bio-Molecules (ITbM), Nagoya University, for kindly teaching me some techniques for my research.

To Dr. Daisuke Ono from the Graduate School of Medicine, Nagoya University, for teaching performance and calculating the dual luminescence.

To Japanese Government (Japanese Ministry of Education, Culture, Sports, Science and Technology; MEXT) scholarship for giving me with the scholarship that allowed me to enroll in a doctoral program.

To Professor Dr. Suriya Sawanon and Dr. Sutisa Majarune from the Department of Animal Science, Faculty of Agricultural at Kamphaeng Saen, Kasetsart University for their recommendation and encouragement to apply for a Japanese Government (MEXT) scholarship.

To all the past and present of the Yoshimura Laboratory members for their friendship and the intelligent discussions that contributed to my development.

Eventually, I would like to express my gratitude to my family members for their always kindly support and understanding.

Abstract

Circadian rhythms are biological oscillations of physical, mental, and behavioral activities with a period of approximately 24 hours driven by an endogenous cell-autonomous timing system called the circadian clock. The current molecular models of the mammalian circadian clocks are based on a molecular mechanism regulated by a transcriptional-translational negative feedback loop (TTFL) in which the translational products of clock genes repress transcription of their own mRNA. Consistent with this model, transcriptional and translational products of *Period*, *Cryptochrome*, and *Bmal1* show circadian rhythm in their accumulation. However, several studies have revealed that constitutively expressed clock genes effectively restore circadian oscillations. To understand this point more quantitatively, I expressed *Bmal1* from a doxycycline (DOX)-inducible promoter in *Bmal1*-disrupted U2OS cells containing a luciferase reporter under the control of the *Bmal1* promoter (P_{Bmal1}), and followed the P_{Bmal1} and P_{Per2} activities. In the presence of DOX at 0.1 and 1 μg/mL, constitutively expressed BMAL1 restored circadian oscillation in P_{Bmal1} and P_{Per2} activities as well as the antiphase relationship between P_{Bmal1} and P_{Per2} oscillations, although the level of BMAL1 and other clock proteins, REV-ERBα and CLOCK proteins showed no clear rhythmicity. I applied a transient response analysis to P_{Bmal1} luminescence data in the presence of various concentrations of doxycycline and found that a slightly damped linear oscillator system can reproduce P_{Bmal1} activity. The oscillation parameters were not dramatically impacted by the amounts of *Bmal1* expression, however, the behavior of the baseline of oscillation was greatly impacted. Based on the obtained transfer functions, this study suggests that BMAL1 is not directly involved in the oscillatory process but modulates the robustness of the oscillations by regulating the basal activity of the clock gene promoter.

Table of Contents

Introduction

Circadian rhythms are biological oscillations of physical, mental, and behavioral activities, such as sleep/wake cycles, metabolisms, and hormone secretion, with an approximately 24 hour periods (Rijio and Takahashi, 2019). These rhythms are controlled by the circadian clock (Serin and Acar Tek, 2019). The term circadian is derived from "circa" which means "approximately" and "dian" which means "day" (Buhr and Takahashi, 2013). Circadian rhythms are adaptive physiological responses that enable organisms to anticipate changes in the 24 hour cycles of light and dark (Takahashi, 2017). Exogenous stimuli, commonly known as zeitgebers or time givers, can entrain organisms to the 24 hour cycles, including light, temperature, and nutrition (Brenna and Albrecht, 2020)

The mammalian circadian system is organized in a hierarchical manner, in which a master pacemaker in the suprachiasmatic nucleus (SCN) of the anterior hypothalamus regulates downstream oscillators in peripheral tissues (Ko and Takahashi, 2006). The SCN contains approximately 20,000 timekeeping neurons and each of which is sensitive to exogenous light stimuli (Reppert and Weaver, 2002). The SCN synchronizes circadian oscillation in almost all cells and organs in the body such as the heart, lung, and liver (Fagiani et al., 2022).

Currently, the molecular model of the circadian clock is based on a mechanism regulated by a cell-autonomous transcriptional-translational negative feedback loop (TTFL) in which the translational products of clock genes repress transcription of their own mRNA (Figure 1). In mammals, the circadian clock consists of an essential core loop and subsidiary ROR/REV/Bmal1 loop coupled to each other, called the interlocked TTFLs, and generates a stable circadian oscillation. In the core loop, circadian locomotor output cycles kaput (CLOCK) and aryl hydrocarbon receptor nuclear translocator-like protein 1 (ARNTL1), commonly known as BMAL1, form CLOCK-BMAL1 heterodimer and activate transcription of *Period* (*Per1* and *Per2*) and *Cryptochrome* (*Cry1* and *Cry2*). This complex binds to a transcriptional

element called Enhancer-box (E-box) in promoter regions and promotes the transcription of *Per* and *Cry*. After a period of time, translational products of *Per* and *Cry* form a heterodimer, phosphorylated, and translocated into the nucleus. In the nucleus, PER and CRY proteins directly interact with CLOCK-BMAL1 heterodimer in order to inhibit the transcription of *Per* and *Cry* (Griffin et al., 1999). PER and CRY proteins thus interfere with this positive drive on *Per* and *Cry* transcription by CLOCK-BMAL1. Both activation and repression are accompanied by extensive changes in posttranslational modification of histones surrounding the transcriptional regulatory region (Brown, 2011), and the stability and the activity of these clock proteins are also controlled by posttranslational modification (Kojima et al., 2011). The cycle starts again, forming a negative feedback loop that generates 24 hour cycles of gene expression that affect the behavior and physiology.

In the ROR/REV/*Bmal1* loop, The CLOCK-BMAL1 heterodimer activates the expression of other transcription factors called ROR (RORα, RORβ, and RORγ) and REV-ERB (REV-ERBα and REV-ERBβ), which oscillates in a circadian manner. These transcription factors control *Bmal1* transcription at ROR Response Elements (RORE). RORs activate *Bmal1* transcription, whereas the REV-ERB protein represses it (Guillaumond et al., 2005, Ko and Takahashi, 2006), which results in BMAL1 protein indirectly controlling transcription of its own mRNA. RORs and REV-ERBs act in the ROR/REV/*Bmal1* loop to support the core loop to maintain its robust oscillation (Ueda et al., 2005). REV-ERB protein can also bind to a response element called the d-site of albumin promoter (D-box) and control the expression of other genes. These transcription factors and response elements affect not only the circadian clock, but also the expression of many additional target genes, called clock-controlled genes, whose promoter regions have E-boxes, ROREs, or D-boxes (Bozek et al., 2009).

Therefore, in the current TTFL models, the oscillation in the levels of transcriptional and translational products of clock genes is necessary to generate circadian oscillation (Ripperger et al., 2000; Griffin et al., 1999; Kume et al., 1999). However, several research revealed that the rhythmicity of clock gene expression is not required, although the genes themselves are necessary for the circadian clock. BMAL1 protein expressed constitutively could restore circadian rhythmicity of *Bmal1*$^{-/-}$ fibroblast cells, suggesting that the rhythm of BMAL1 protein is not necessary for the basic core loop (Liu et al., 2008). The cell-permeant CRY1 and CRY2 proteins can rescue circadian properties in *Cry1*$^{-/-}$*Cry2*$^{-/-}$ mouse fibroblasts (Fan et al., 2007). These studies revealed that cycling of CRY1, CRY2, and BMAL1 is not necessary for circadian clock function in fibroblasts. Constitutively expressed *Per2* from an artificial promoter also restored rhythmicity in arrhythmic *Per1*$^{-/-}$ and *Per2*$^{-/-}$ mice *in vivo* and *in vitro* (Alessandro et al., 2015). In the present TTFL model, post-translational modification also plays an important role (Geo and Kannan, 2021). Modifications of clock proteins regulate their stability, interaction with other proteins, and subcellular localization (Okamoto-Uchida et al., 2019). Modification of clock proteins imposes a substantial delay between the accumulation of clock genes mRNA and its mature protein products to adjust the period of the oscillation to 24 hours. However, how and why the constitutive expression of clock genes can restore circadian oscillation is still not fully understood.

The objective of this study is to investigate quantitatively how the *Bmal1* constitutive expression affects circadian oscillations. I focused on *Bmal1* because *Bmal1* is the only circadian clock gene whose single deletion disrupts the mammalian circadian clock system (Haque et al., 2019). Here, I established a novel cellular system for studying the effects of constitutively expressed BMAL1 on P_{Bmal1} activity using the firefly luciferase gene (*Fluc*) as a reporter. I inactivated endogenous *Bmal1* by CRISPR-Cas9 method in human U2OS cells containing a reporter of *Bmal1* promoter (P_{Bmal1}::*Fluc*), and stably introduced an exogenous

gene coding Myc-tagged BMAL1 (MYC-BMAL1) driven by a non-rhythmic, doxycycline (DOX)-inducible promoter. Using cell lines thus obtained, I investigated the effect of constitutively expressed Myc-BMAL1 on P_{Bmal1} and P_{Per2} activities, and on the accumulation of the proteins involved in ROR/REV/*Bmal1* loop. Finally, I performed transient response analysis to obtain transfer function models that recapitulate the behavior of P_{Bmal1} activity under the various levels of MYC-BMAL1.

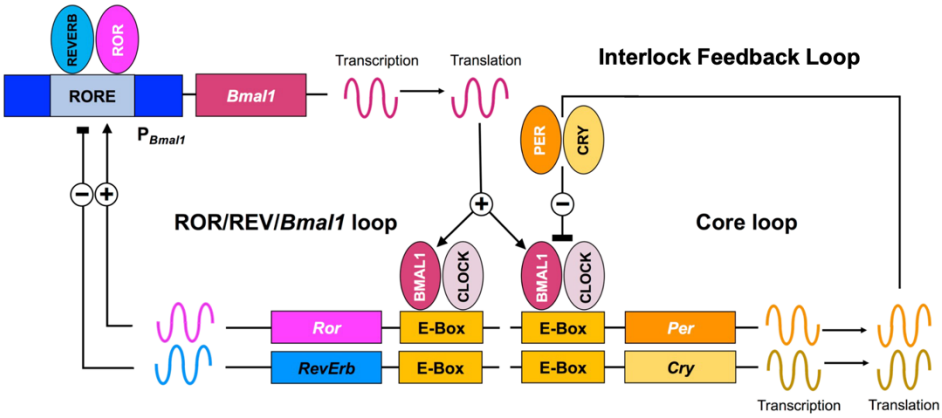

Figure 1. Transcriptional-translational negative feedback loop (TTFL) model of the molecular circadian clock in mammals.

Materials and Methods

Construction of doxycycline-inducible expression plasmid of Myc-BMAL1

The human *Bmal1* ORF was amplified by PCR using KOD-plus-neo (Toyobo Biotechnology, Osaka, Japan) from the Kazusa Flexi ORF clone FXC03462 (Promega, Madison, WI) using the following primers: Bmal1ORF_fwd, 5' CCGGAATTCATGGCAGACCAGAGAATGGACATTTCT 3'; Bmal1ORF_rev, 5' CGCGGATCCTCACAGCGGCCATGGCAAGTCACTAAAGTC 3'. The PCR product was digested with EcoRI and BamHI and cloned into the EcoRI-BamHI site of pTetOne (Takara Bio USA, San Jose, CA). The Myc-tag was introduced into the resultant plasmid by inverse PCR using the KOD-Plus mutagenesis kit, according to the manufacturer's instructions. The following primers were used for inverse PCR: Myc-Bmal1_fwd, 5' ACCATGGAGCAGAAGCTGATCTCAGAGGAGGACCTGATGGCAGACCAGAGAAT GGACATTTCT 3'; Myc-Bmal1_rev, 5' GAATTCTTTACGAGGGTAGGAAGTGGT 3'. The resulting plasmid was named pTetOne-MycBmal1.

Purification of plasmid DNA

For purification of plasmid DNA, firstly transformation of *E. coli* was performed by adding 1 μL of plasmid solution to 100 μL of DH5α competent cells on ice (less than 5% of competent cells in volume) and mixing by pipetting only once. Then, competent cells were incubated on ice for 5 minutes, heat-shocked at 42°C for 30 seconds, and incubated on ice for 2 minutes. Cells were then pipetted into 900 μL of SOC medium and incubated at 37°C with shaking at 200 rpm. The *E. coli* culture was plated onto LB plates at 20 and 200 μL, and the plates were incubated at 37°C with upside down overnight. The next morning, a single colony was picked up from a plate using a toothpick and put into 2 mL of medium, then incubated at 37°C with shaking at 200 rpm for 8 hours. After that, 100 μL of preculture was put into 100

mL of LB medium and incubated at 37°C with shaking at 200 rpm overnight. The *E. coli* culture was pelleted for purification of plasmid DNA using the QIAGEN Plasmid Maxi kit (QIAGEN, Venlo, Netherland) following the manufacturer's instructions. The pellet of DNA thus obtained was dissolved in TE buffer (10 mM Tris, pH 8.0, 0.1 mM EDTA), measured the concentration by spectrophotometer (DS-11; Denovix, Wilmington, DE). and stored at -20°C until use.

Disruption of *BMAL1* in U2OS-P$_{Bmal1}$::*Fluc* cells

Human U2OS cells (HTB-96; American Type Culture Collection, Manassas, VA) containing the P$_{Bmal1}$::*Fluc* reporter (U2OS-P$_{Bmal1}$::*Fluc*) (Oshima et al, 2015) were plated onto the 35 mm culture dishes (Nunc EasYDish; Thermo Fisher Scientific, Waltham, MA) at a density of 2×10^5 cells/dish in Dulbecco's modified Eagle's medium (DMEM) (D6429; Sigma-Aldrich, St. Louis, MO) supplemented with 10% fetal bovine serum, 2 mM of glutamine, 100 units/mL of penicillin, and 100 μg/mL of streptomycin and cultured at 37°C with 10% CO_2 for approximately 24 hours.

U2OS-P$_{Bmal1}$::*Fluc* was transfected with 1.4 μg of human *BMAL1* CRISPR/Cas9 KO plasmid (sc-400808; Santa Cruz Biotechnology, Dallas, TX, USA), consisting of a pool of three plasmids, each encoding the Cas9 nuclease and a target-specific 20 nt guide RNA (sgA, sgB, and sgC), and 1.4 μg of human *BMAL1* HDR plasmid (sc-400808-HDR; Santa Cruz Biotechnology, Dallas, TX), using Xfect transfection reagent (Takara Bio USA, San Jose, CA) following the manufacturer's instructions. Puromycin-resistant clones were selected in the presence of puromycin at 1 μg/mL. *Bmal1* knockout clones were screened by immunoblot analysis using an anti-BMAL1 (B-1; Santa Cruz Biotechnology, Dallas, TX, USA), and confirmed by genomic PCR followed by Sanger sequencing. The DNA sequence of the human ARNTL gene (ID 408), a synonym of *BMAL1*, was obtained from the GenBank database, and

used as a reference sequence. The following primers were used for genomic PCR and Sanger sequencing: C_fwd, 5' AGATCATCCAATGGCAGAC 3'; C_rev:5' GAGATGACACCCATAGACTTA 3'; B_fwd:5' AAGAAGCTCTTCTGTATGTC 3"; B_rev:5' AATAAGGTCCAAGCTTACCT 3'; A_fwd:5' AAGAGCGATGTCGTTGGAG 3"; A_rev:5' TGCATGGTACAAGTCCTGAAGC 3' (Figure 2). The *Bmal1* knockout clone, named U2OS-P$_{Bmal1}$::*Fluc*/Δ*Bmal1*, was used to establish the Myc-tagged BMAL1 (MYC-BMAL1) inducible clones.

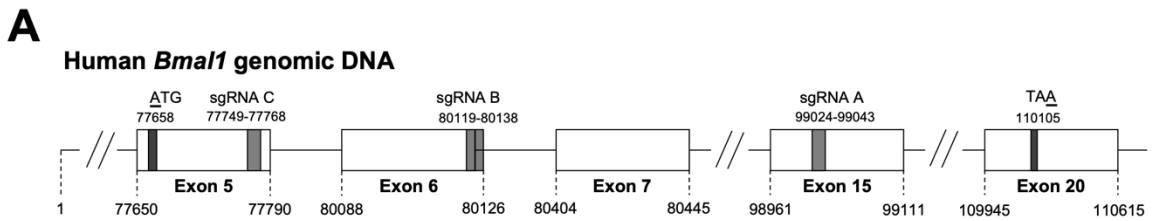

B

Primers		Amplicon size (bp)		
Forward primer	Reverse primer	Predicted	ΔBmal1	
C_fwd	C_rev	496	No Amp	
C_fwd	B_rev	2816	446	➡ Amplicon BC
C_fwd	A_rev	21663	361	➡ Amplicon AC

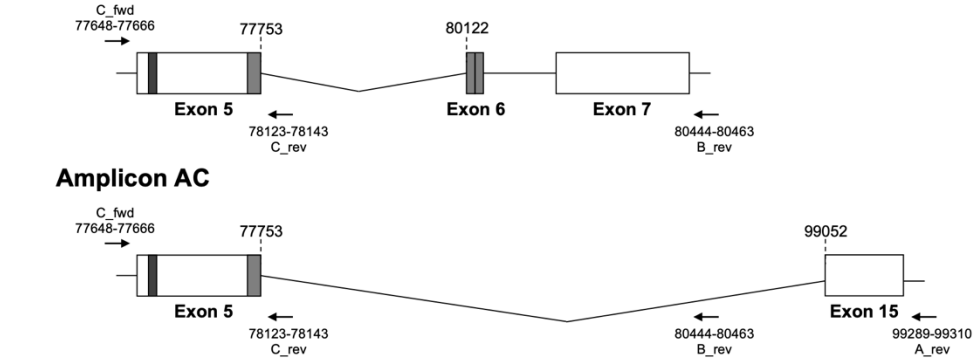

D

Amplicon BC

AGATCATCCAATGGCAGACCAGAGAATGGACATTTCTTCAACCATCAGTGATTTCATGTCCCCGGGCCCCACCGA
CCTGCTTTCCAGCTCTCTTGGTACCAGTGGGAAGGTACCATTGAACCTAGTAATTTGAACTTCAGCATCCTTATAG
CCATTTTCTTTGCACTGTTACACATTCTGTTACTTGGGGCAGCACCCATGTCCTCAACTGGAGATGAGCAAGGAG
GCCGTGAGCCTGTGGGCGCTCACTGTGTCCCTCCAACCCCCAGTCCCCTTGTGTGTCTGCAGAGAGATGACAGGA
TCAGGCAGAAGAAAACAGCAATGTGTAACTTTGCCATTCATCTCCAGAGAATTATGTTTTTATCTTTTGCTTTTTC
CTCCCCAGGTTAGAATATACAGAACACCAAGGAAGGATAAAAAATGCAAGGTAAGCTTGGACCTTATT

E

Amplicon AC

AGATCATCCAATGGCAGACCAGAGAATGACATTTCTTCAACCATCAGTGATTTCATGTCCCCGGGCCCCACCGAC
CTGCTTTCCAGCTCTCTTGGTACCAGTTTCATGAACCCTTGGACCAAGGAAGTAGAATATATTGTCTCAACTAAC
ACTGTTGTTTTGTAAGTACTTTTCCTATATCTGAAGCTCCCCTGCTTCAAACAGATGCCTAGGGTTCCTCATCTGG
GAAATGGGGTGCAGGCAACATCCAGTATCACATCCTTTAATGCCATCTTGCTAATACCTGTGGAAGCCTCAGGAC
TGGCAGAAGCTAGAAAGGATTGTAACAAAGGGACAAGCTTCAGGACTTGTACCATGCA

Figure 2. (A) Schematic diagram of the human *BMAL1* gene. The DNA sequence of the human ARNTL gene (ID 408), a synonym of *BMAL1*, was obtained from the GenBank database. The positions of the sgRNAs and the start and stop codons are shown in the figure. (B) Results of genomic PCR analysis of the regions flanking the sgRNA-binding sites. Genomic DNA was prepared from U2OS-P$_{Bmal1}$::*Fluc*/Δ*Bmal1* cells and was subjected to PCR using the indicated

primers. Amplicon sizes predicted from the database (predicted) and those obtained from the experiment (Δ*Bmal1*) are shown. No amplification was observed using C_fwd and C_rev primers. (C) Schematic diagram of amplicons BC and AC. The primer positions are shown by arrows. Nucleotides 77753 to 80112 and 77751 to 99052 were deleted in amplicons BC and AC, respectively. (D, E) DNA sequences of amplicons BC (D) and AC (E) were determined by direct Sanger sequencing of the amplicons.

Establishment of MYC-BMAL1 inducible cell lines

U2OS-P$_{Bmal1}$::*Fluc*/Δ*Bmal1* cells were plated onto the 35 mm culture dish (Nunc EasYDish; Thermo Fisher Scientific, Waltham, MA) at a density of 2 × 10^5 cells/dish in Dulbecco's Modified Eagle's Medium (DMEM) (D6429; Sigma-Aldrich, St. Louis, MO) supplemented with 10% fetal bovine serum, 2 mM of glutamine, 100 units/mL of penicillin, and 100 μg/mL of streptomycin, and cultured at 37°C with 10% CO_2 for approximately 24 hours. Then cells were transfected with 5 μg of pTetOne-MycBmal1 plasmid and 0.25 μg of linear hygromycin marker (Takara Bio USA, San Jose, CA) using the Xfect transfection reagent (Takara Bio USA, San Jose, CA). After 48 hours of transfection, trypsinize and replate the cells at various densities as follows; 1/4, 1/8, 1/16, 1/32, 1/64, 1/128, 1/256, and 1/512 onto the 10 cm dish at duplicates for each condition. For antibiotic selection, 300 μg/mL of Hygromycin B was added to the cell cultures to select positive clones. MYC-BMAL1 protein expression in the isolated clones was evaluated by immunoblot analysis using an anti-Myc-tag mAb (My3, MBL) in the presence of Doxycycline (DOX) 1 μg/mL (Takara Bio USA, San Jose, CA). The seven cell lines named U2OS-P$_{Bmal1}$::*Fluc*/Δ*Bmal1*/P$_{TRE3Gs}$::*Myc-Bmal1* strains-2,-17, -23, -27, -33, -51, and -59 were obtained.

Luminescence measurement

For single reporter measurement, U2OS-P$_{Bmal1}$::*Fluc*/Δ*Bmal1*/P$_{TRE3Gs}$::*Myc-Bmal1* strains were plated at a density of 8 × 10^3 cells/well onto the 96 well white culture plates with a clear bottom (IsoPlate^{TM} – 96TC, PerkinElmer, Waltham, MA) and cultured for 48 hours at 37°C with 10% CO_2 to reach confluence. Cells were treated at various concentrations of DOX from 0 to 10 μg/mL and continued to culture for another 48 hours. Then, the medium was changed to that for luminescence measurement; DMEM (D2902, Sigma-Aldrich, St. Louis, MO) supplemented with 3.5 mg/mL of D-glucose, 0.35 mg/mL of $NaHCO_3$, 2% B-27 (Gibco),

2 mM of glutamine, 100 units/mL of penicillin, 100 μg/mL of streptomycin, 0.1 mM of D-luciferin, 100 nM of dexamethasone, and DOX with the same concentrations as previous, and luminescence was measured every 20 minutes for 6 days using a plate reader (Enspire; PerkinElmer, Waltham, MA). An integration time of 1 second was employed for each measurement.

For dual reporter measurement, U2OS cells or U2OS-P$_{Bmal1}$::*Fluc*/Δ*Bmal1*/P$_{TRE3Gs}$::*Myc-Bmal1* strain-2 cells were plated onto the 35 mm culture dishes (Nunc EasYDish; Thermo Fisher Scientific, Waltham, MA) at a density of 2×10^5 cells/dish and DOX was added at the various concentrations (0, 0.01, 0.1, 1, and 10 μg/mL) onto U2OS-P$_{Bmal1}$::*Fluc*/Δ*Bmal1*/ P$_{TRE3Gs}$::*Myc-Bmal1* strain-2 cells only. On the next day, U2OS cells were transiently transfected with either 2.5 μg of pP$_{Bmal1}$::*Fluc* plasmid containing a 530 bp fragment of mouse *Bmal1* promoter region (Kiyohara et al., 2006) at the SacI-XhoI site of pGL4.11[luc2P] (Promega, Madison, WI) or 2.5 μg of pP$_{Per2}$::*Eluc* plasmid containing a 423 bp fragment of the mouse *Per2* promoter region (Kiyohara et al., 2006) at the BglII-EcoRI site of pEluc(PEST)-test (Toyobo Biotechnology, Osaka, Japan) as a control, and U2OS-P$_{Bmal1}$::*Fluc*/Δ*Bmal1*/P$_{TRE3Gs}$::*Myc-Bmal1* strain-2 cells were transiently transfected with 2.5 μg of pP$_{Per2}$::*Eluc* plasmid using the Xfect transfection reagent (Takara Bio USA, San Jose, CA), and incubated for another 24 hours. The medium was changed to that for luminescence measurement supplemented with DOX at the same concentrations, and luminescence from P$_{Bmal1}$::*Fluc* and P$_{Per2}$::*Eluc* reporters was measured simultaneously using Kronos-Dio (ATTO, Tokyo, Japan), equipped with a 600 nm long pass filter, for 6 days according to the method described by Ono et al (2016).

Preparation of samples for immunoblot analysis

Wild-type U2OS cells containing the P_{Bmal1}::*Fluc* reporter (U2OS-P_{Bmal1}::*Fluc*) and U20S-P_{Bmal1}::*Fluc*/Δ*Bmal1*/P_{TRE3Gs}::*Myc-Bmal1* strain-2 cells were plated onto the 35 mm culture dishes (Nunc EasYDish; Thermo Fisher Scientific, Waltham, MA) at a density of 2 × 10^5 cells/dish and cultured in DMEM (D6429; Sigma-Aldrich, St. Louis, MO) supplemented with 10% fetal bovine serum, 2 mM of glutamine, 100 units/mL of penicillin, and 100 μg/mL of streptomycin at 37°C with 10% CO_2. When cells reached confluence (2 to 3 days later), DOX was added at various concentrations (0, 0.01, 0.1, 1, and 10 μg/mL) and continued to be cultured for another 48 hours. Then, the medium was changed to DMEM (D6429; Sigma-Aldrich, St. Louis, MO) supplemented with 2% B-27 (Gibco), 2 mM of glutamine, 100 units/mL of penicillin, 100 μg/mL of streptomycin, 100 nM of dexamethasone, and DOX was added at the same previous concentration. Cells were then lysed with 1 × SDS sample buffer (BioRad, Hercules, CA) from 0 to 52 hours every 4 hours interval after the addition of dexamethasone. Samples were sonicated using a Bioruptor UCW 310 (Cosmo Bio, Tokyo, Japan) at 30 seconds on, 30 seconds off, 25 times at 310 W in cold water (4°C). The samples were centrifuged at 20,000 × *g* for 10 minutes at 4°C to remove debris and denatured at 95°C for 5 minutes. Protein concentration was measured by Pierce 660 nm Protein Assay Reagent (Thermo Fisher Scientific, Waltham, MA) using bovine serum albumin (BSA) as a standard (Table 1). Samples were diluted if necessary. Then, 10 μL of samples or standards were mixed with 150 μL working reagent in a 1.5 mL tube, incubated for 5 minutes at room temperature, and were moved to a 96 well plate to measure absorbance at 660 nm using a plate reader (EnSpire; PerkinElmer, Waltham, MA).

Table 1. The standard of protein concentrations

Concentration (mg/mL)	2 mg/mL BSA (μL)	1 × SDS sample buffer (μL)	MilliQ (μL)
1.0	20	20	0
0.8	16	20	4
0.6	12	20	8
0.4	8	20	12
0.2	4	20	16
0	0	20	20

Immunoblot analysis of circadian clock proteins

Protein samples of U2OS-P$_{Bmal1}$::*Fluc*/Δ*Bmal1*/P$_{TRE3Gs}$::*Myc-Bmal1* strain-2 cells were separated by SDS-PAGE on 7.5% gels (E-R7.5L, ATTO, Tokyo, Japan) loaded at 20 μg/lane and transferred to polyvinylidene difluoride (PVDF) membranes using the iBlot 2 Dry Blotting system (Thermo Fisher Scientific, Waltham, MA). For U2OS-P$_{Bmal1}$::*Fluc*, protein samples were separated by SDS-PAGE on 10% polyacrylamide gels (10% T, 0.67% C) and blotting was performed by a semi-dry blotting apparatus (4M-R, ATTO, Tokyo, Japan) at 2 mA/cm^2 for 1 hour. After blotting, the membranes were washed twice with MilliQ for 5 minutes. Then, membranes were stained with Ez Stain Aqua Mem solution (ATTO, Tokyo, Japan) to measure total protein levels. For total protein staining, the membranes were soaked in the Wash solution, and shaking for 5 minutes at room temperature. Then, the membranes were soaked in Stain solution for 5 minutes at room temperature, De-stain solution twice for 5 minutes at room temperature, and remove the residual solution completely with a paper towel. The membrane images were captured using LuminoGraph II EM (ATTO, Tokyo, Japan) in bright field mode. After that, the membranes were soaked in Bleach solution for 5 minutes at room temperature, then the membranes were washed twice with MilliQ for 5 minutes and then washed with Tris-buffered saline containing 0.2% Tween 20 (TBS-T) three times for 5 minutes each with shaking.

Membranes were blocked overnight with 5% skim milk dissolved in TBS-T at 4°C. The membranes were incubated with primary antibody diluted in 5% skim milk in TBS-T for 1.5 hours at room temperature and washed three times with TBS-T for 10 minutes. The membranes were incubated with secondary antibody for 1.5 hours at room temperature and washed three times with TBS-T for 10 minutes. For luminescence detection, membranes were treated with ECL prime (Cytiva, Marlborough, MA) according to the manufacturer's instructions, and signals were captured using the LuminoGraph II EM (ATTO, Tokyo, Japan). Quantification of band intensity was performed using the Image J software (NIH, USA). The background signal was measured in a signal-free area of the membrane and subtracted from the intensity of each band, which was then normalized by total protein.

The antibodies used and their dilutions were as follows: anti-Myc-tag mAb (My3; MBL, Tokyo, Japan), 1:200; anti-REV-ERBα pAb (NR1D1) (PM092; MBL, Tokyo, Japan), 1:200; anti-CLOCK (18094-1-AP; Proteintech, Chicago, IL), 1:500; anti-ARNTL (14268-1-AP; Proteintech, Chicago, IL), 1:3000; HRP-linked anti-mouse IgG (NA931; Cytiva, Marlborough, MA), 1:1000; and HRP-linked anti-rabbit IgG (NA934; Cytiva, Marlborough, MA), 1:1000.

Quantitative reverse transcription PCR (RT-PCR)

U2OS-P$_{Bmal1}$::*Fluc* and P$_{Bmal1}$::*Fluc*/Δ*Bmal1*/P$_{TRE3Gs}$::*Myc-Bmal1* strain-2 cells were plated onto the 35 mm culture dishes (Nunc EasYDish; Thermo Fisher Scientific, Waltham, MA) at a density of 2×10^5 cells/dish and cultured in DMEM (D6429; Sigma-Aldrich, St. Louis, MO) supplemented with 10% fetal bovine serum, 2 mM of glutamine, 100 units/mL of penicillin, and 100 μg/mL of streptomycin at 37°C with 10% CO_2. When cells reached confluence (2 to 3 days later), DOX was added at the various concentrations (0, 0.01, 0.1, 1, and 10 μg/mL) and continued to be cultured for another 48 hours. Then, the medium was changed to DMEM supplemented with 2% B-27 (Gibco), 2 mM of glutamine, 100 units/mL of

penicillin, 100 μg/mL of streptomycin, 100 nM of dexamethasone, and DOX was added at the same previous concentration. The time-series samples for quantitative RT-PCR were collected from 24 to 52 hours after the addition of dexamethasone at 4 hours interval. Total RNA was extracted using the RNeasy-plus micro kit (QIAGEN, Venlo, Netherland) following the manufacturer's instructions and total RNA concentration was measured using a spectrophotometer (DS-11; Denovix, Wilmington, DE). Reverse transcription was performed using ReverTra Ace (Toyobo Biotechnology, Osaka, Japan) at 3 μg of total RNA. Quantitative RT-PCR reaction was performed using QuantStudio 3 (Applied Biosystems, Waltham, MA) in 20 μL of a reaction mixture containing 10 μL of 2 × TaqMan gene expression master mix (Applied Biosystems, Waltham, MA), 4 μL of the reverse transcription reaction mixture, and 1 μL of 20 × TaqMan gene expression assay (HS01587195_m1 for *BMAL1* and HS02786624_g1 for *GAPDH*, Applied Biosystems, Waltham, MA). Relative expression was calculated using Pfaffl's method (Pfaffl, 2001) with *GAPDH* as an internal control.

Statistical analysis

Statistical analysis was conducted using GraphPad Prism version 7.0 (GraphPad Software, San Diego, CA, USA). The significance of differences was analyzed using one-way analysis of variance (ANOVA) followed by Tukey's multiple comparison tests. Values are expressed as mean ± standard error (SEM). Rhythmicity was determined using the JTK cycle test (Hughes et al., 2010). All *P*-values were from two-tailed tests, and values less than 0.05 were considered statistically significant.

Results

BMAL1 expressed from inducible promoter can restore rhythmicity of P_{Bmal1} activity

Novel P_{Bmal1}::*Fluc* reporter cell lines in which endogenous *Bmal1* is inactivated and Myc-tagged BMAL1 (MYC-BMAL1) is expressed under a DOX-inducible promoter P_{TRE3Gs} were established as follows: *Bmal1* in wild-type U2OS containing P_{Bmal1}::*Fluc* reporter (U2OS-P_{Bmal1}::*Fluc*) was inactivated by CRISPR-Cas9 to obtain U2OS-P_{Bmal1}::*Fluc*/Bmal1 KO. This cell line was stably transfected with pTetOne-MycBmal1 plasmid, and seven strains named U2OS-P_{Bmal1}::*Fluc*/Δ*Bmal1*/P_{TRE3Gs}::*Myc-Bmal1* strains-2, -17, -23, -27, -33, -51, and -59 were obtained (Figure 3). I measured the luminescence from P_{Bmal1}::*Fluc* in the presence of DOX at 0, 0.01, 0.1, 1, and 10 μg/mL. 100 nM of dexamethasone was added at time 0 for resetting the circadian clock (Beta et al., 2022; Balsalobre et al., 2000), and started the measurement of luminescence. The intensity of luminescence decreased as the concentration of DOX increased (Figure 4), suggesting that BMAL1 inhibits the P_{Bmal1} activity.

Circadian rhythm in P_{Bmal1} activity was clearly restored in strains-2 and -51 in the presence of DOX at 0.1 and 1 μg/mL. Rhythmicity was restored in strains -33 and -59, but not as robustly as in strains -2 and -59. The P_{Bmal1} rhythmicity in strains-17, -23, and -27 was not as robust as these three strains, however, the intensity of luminescence from P_{Bmal1}::*Fluc* was greatly reduced as the DOX concentration increased in all seven strains. Next, I measured the MYC-BMAL1 protein accumulation for explained the robust rhythmicity in the seven cell lines treated with DOX at 0.01 or 1 μg/mL for 2 days before synchronization with dexamethasone (Figure 5). Strain-23 shows the highest of the MYC-BMAL1 protein levels in the presence of DOX at 0.01 (Figure 5A) and 1 μg/mL (Figure 5B). Strain-51 shows weak rhythmicity, even in the presence of DOX at 0.01 μg/mL, which may reflect the slightly higher MYC-BMAL1 protein accumulation compared to strain-2 in the presence of DOX at 0.01 μg/mL. MYC-BMAL1 protein levels were significantly higher in strains-23 and -33 and lower in strains-27

and 33 than in strain-2 in the presence of DOX at 1 μg/mL. Strains-51 and -59 showed no significant differences compared to strain-2. In strain-23, MYC-BMAL1 was three to four-fold higher than in strain-2, while in strain-33, the level was comparable to that in strain-51. These results indicate that appropriate induction levels of MYC-BMAL1 protein are required to restore rhythmicity. Next, strain-2 cells were subjected to further experiments. I added the DOX at various concentrations (0, 0.005, 0.01, 0.02, 0.05, 0.1, 0.2, 0.5, 1, and 10 μg/mL) to U2OS-P_{Bmal1}::*Fluc*/Δ*Bmal1*/P_{TRE3Gs}::*Myc-Bmal1* strain-2 cells in order to confirm whether the circadian rhythm in the luminescence from P_{Bmal1}::*Fluc* reporter was restored by constitutively expressed MYC-BMAL1. Without DOX (0 μg/mL) or in the presence of lower concentrations of DOX (from 0.005 to 0.02 μg/mL), the intensity of luminescence from P_{Bmal1} activity unsteadily fluctuated and weakly oscillated (Figure 6). In the presence of DOX at 0.05 and 0.1 μg/mL, the intensity of luminescence showed clearly damped oscillation with the intensity of luminescence gradually increasing. In the presence of DOX from 0.2 to 1 μg/mL, the intensity of luminescence also showed clearly damped oscillations. The intensity of the luminescence was gradually stabilized at a specific value. In the presence of a high DOX concentration (10 μg/mL), the luminescence converged after one overshoot. The period of the oscillations was calculated to be approximately 25 hours by chi-square periodogram analysis at any DOX concentrations from 0.02 to 10 μg/mL (Figure 7, Table 2). These results suggest that the amount of MYC-BMAL1 affects the baseline and robustness but not the period of the oscillation in P_{Bmal1} activity.

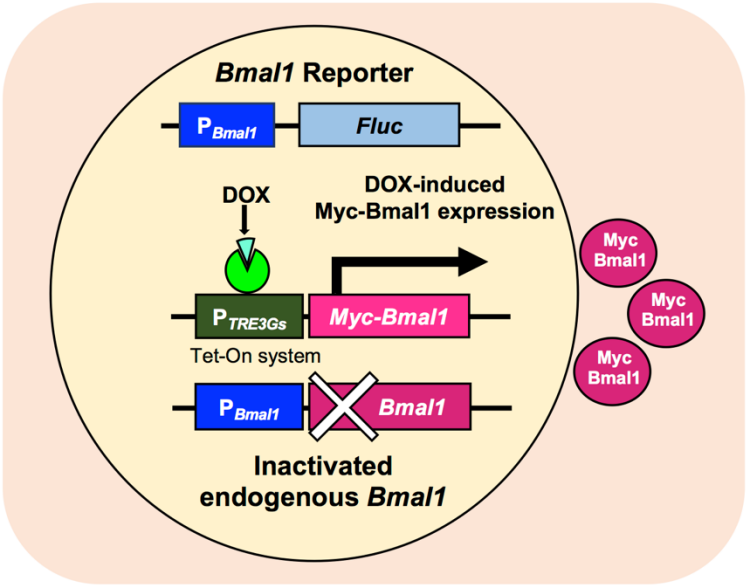

Figure 3. Schematic diagram of U2OS-P$_{Bmal1}$::*Fluc*/Δ*Bmal1*/P$_{TRE3Gs}$::*Myc-Bmal1* strains. Endogenous *Bmal1* was inactivated by CRISPR-Cas9, and a gene coding MYC-BMAL1 was expressed from the DOX-inducible promoter P$_{TRE3Gs}$. *Bmal1* promoter activity was monitored using the P$_{Bmal1}$::*Fluc* reporter.

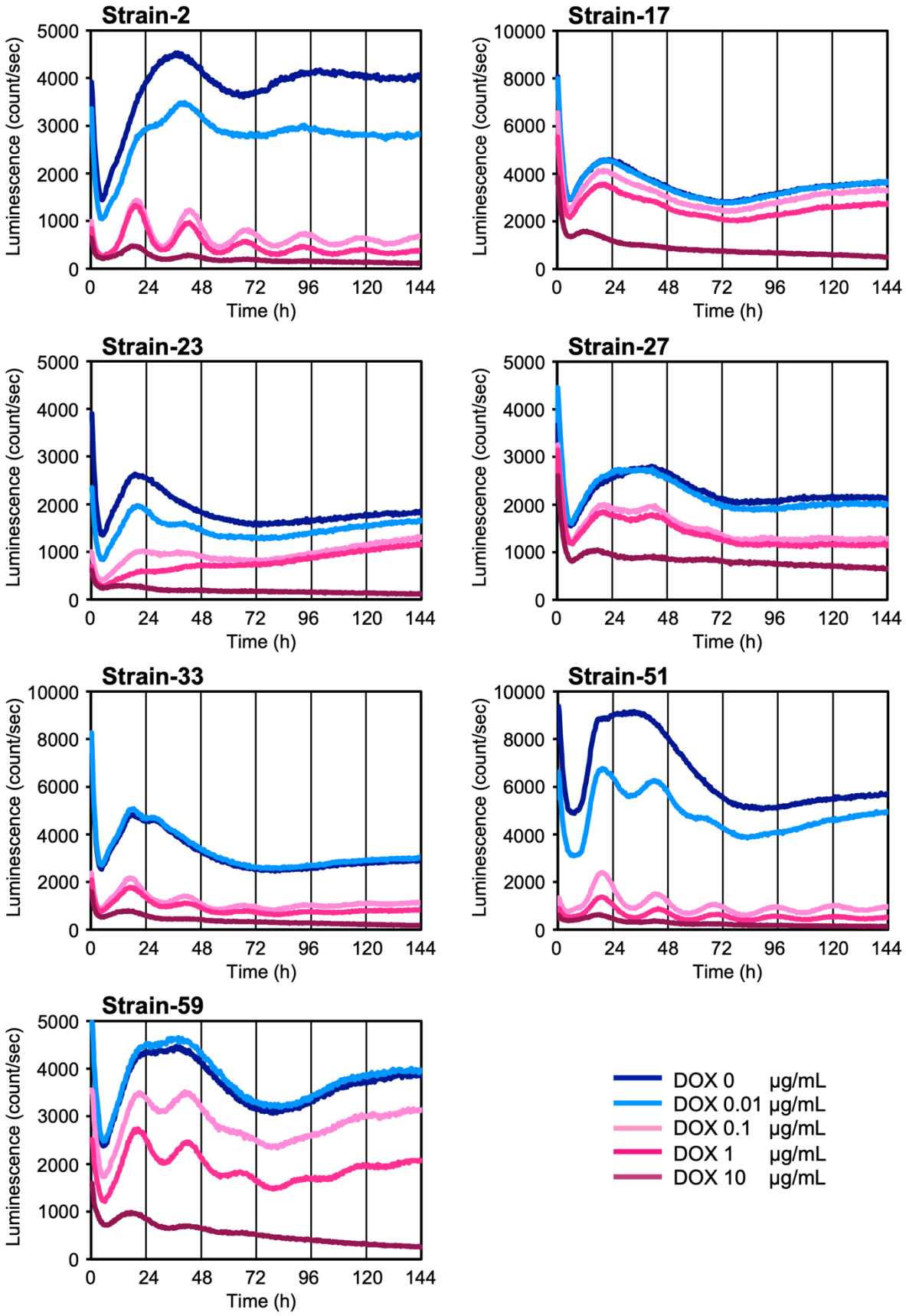
Strain-2
Strain-17
Strain-23
Strain-27
Strain-33
Strain-51
Strain-59
Luminescence (count/sec)
Time (h)
0
24
48
72
96
120
144
DOX 0 μg/mL
DOX 0.01 μg/mL
DOX 0.1 μg/mL
DOX 1 μg/mL
DOX 10 μg/mL

Figure 4. U2OS-P$_{Bmal1}$::*Fluc*/Δ*Bmal1*/P$_{TRE3Gs}$::*Myc-Bmal1* strains-2, -17, -23, -27, -33, -51, and -59 cells were subjected to measurements of P$_{Bmal1}$::*Fluc* reporter luminescence. The average of triplicate measurements is shown. Doxycycline (DOX) concentrations are indicated on the bottom right side of the figure.

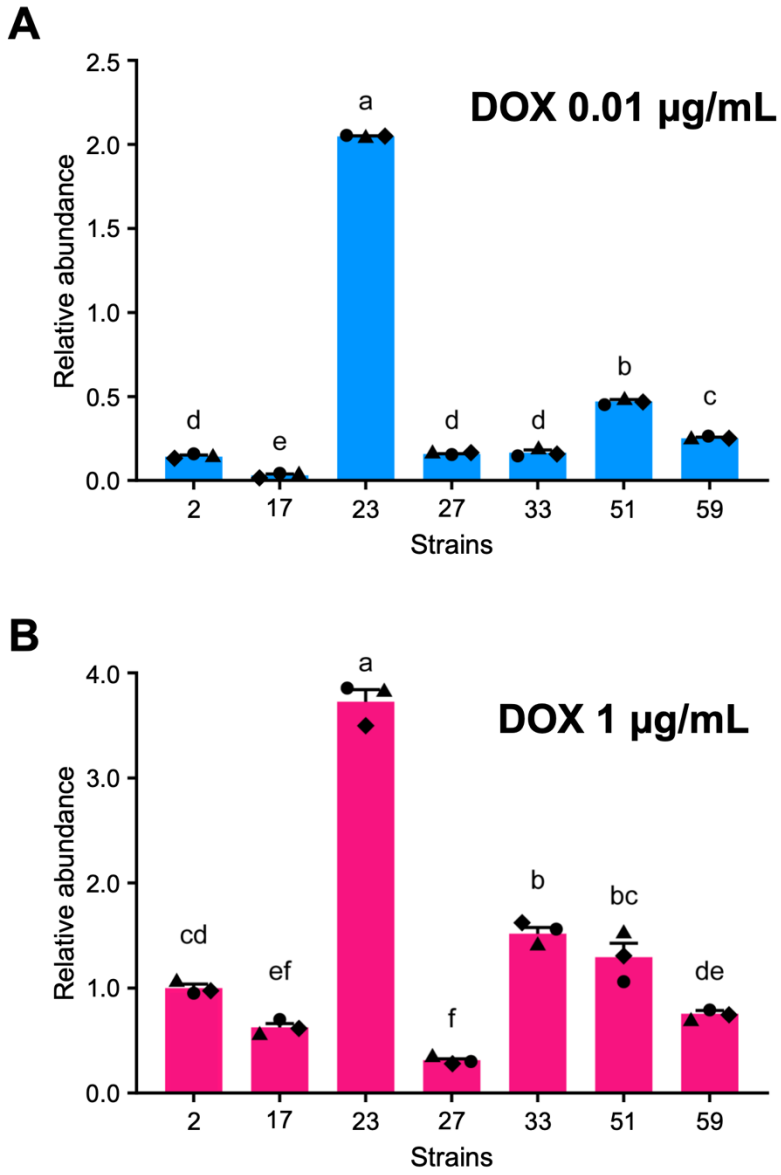

Figure 5. U2OS-P$_{Bmal1}$::*Fluc*/Δ*Bmal1*/P$_{TRE3Gs}$::*Myc-Bmal1* strains-2, -17, -23, -27, -33, -51, and -59 cells were subjected to measurements of MYC-BMAL1 protein levels. Total protein samples were collected from seven cell line strains 48 hours after the addition of doxycycline (DOX) at 0.01 (A) or 1 µg/mL (B). For protein accumulation, equal amounts of the protein samples collected within each DOX concentration were mixed and subjected to immunoblot analysis using an anti-Myc antibody. Results were normalized using the average value of DOX at 1 µg/mL, and data are shown as the mean ± SEM. N = 3 samples/group, one-way ANOVA followed by Tukey's multiple comparison test, different characters (a, b, c, d,

e,f) indicate significant differences ($P < 0.05$). Protein samples were collected and subjected to immunoblot analysis in three independent experiments. Markers (▲,◆, and ●) indicate MYC-BMAL1 in three biological replicates.

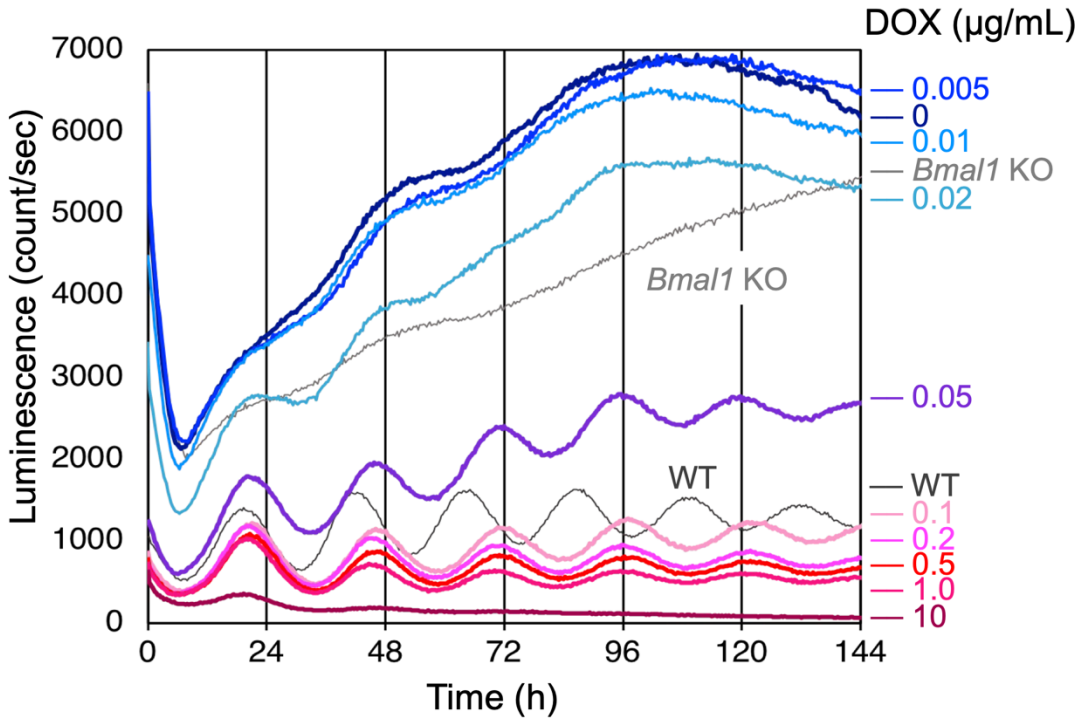

Figure 6. MYC-BMAL1 expressed from a DOX-inducible promoter restores rhythmicity in P_{Bmal1} activity. Time course of the luminescence measurements from the U2OS-P_{Bmal1}::*Fluc*/Δ*Bmal1*/P_{TRE3Gs}::*Myc-Bmal1* strain-2 cells was measured every 20 minutes. Each measurement was taken in triplicate and the average values are shown. DOX concentrations are indicated on the right side of the graph.

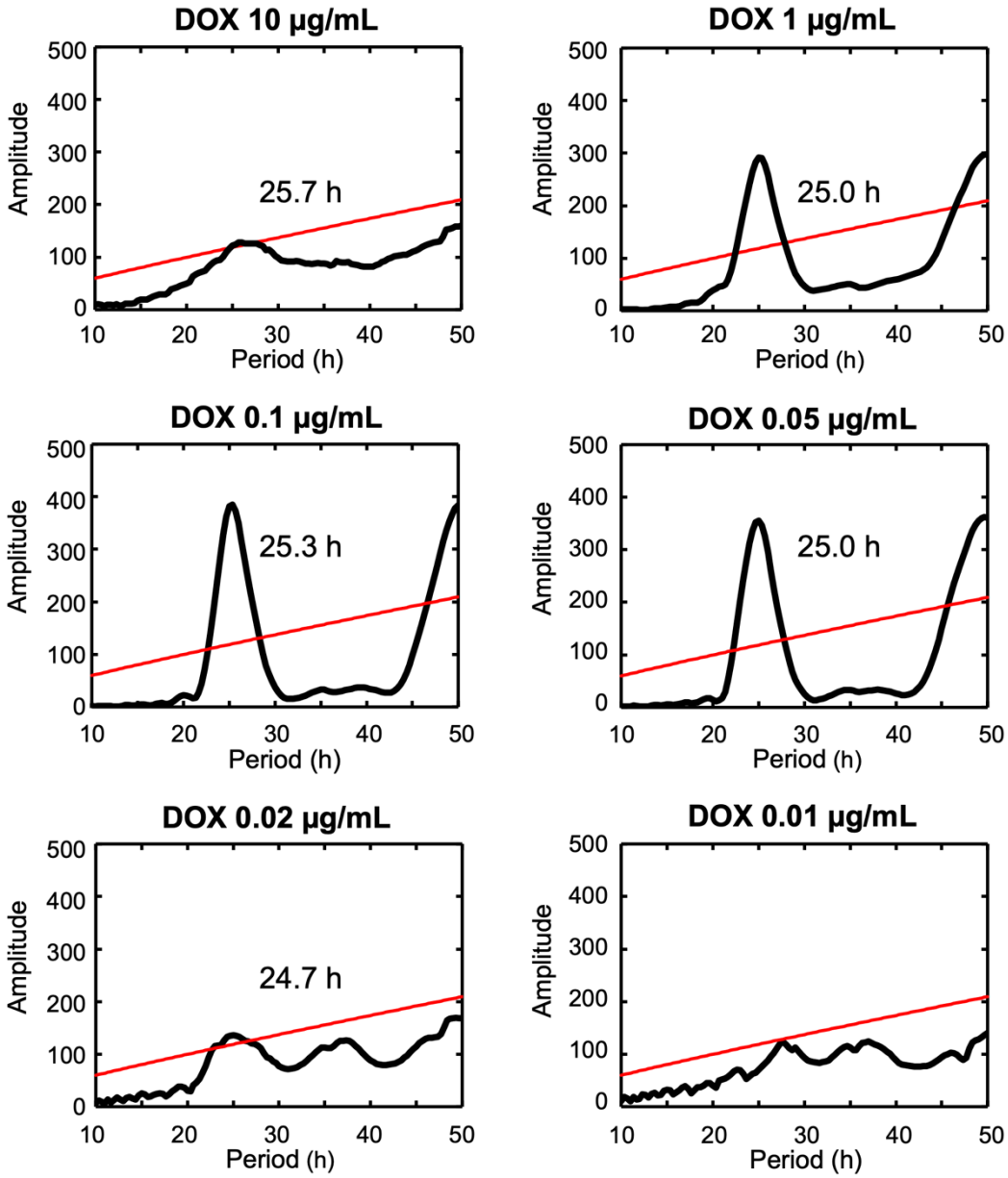

Figure 7. Periodogram analysis shown the period of P$_{Bmal1}$::*Fluc* activity calculated for each DOX concentration. Luminescence data from 0 to 144 hours shown in Figure 6 were subjected to chi-square periodogram analysis using Lumicycle analysis software (ActiMetrics; Wilmette, IL, USA) to assess of their oscillatory component and its significance. The black line shows the period and the red line shows the significance level (P = 0.05).

Table 2. Period of P_{Bmal1}::*Fluc* oscillation calculated for each DOX concentration

DOX concentration (μg/mL)	10	1	0.1	0.05	0.02	0.01
Period (τ) (h)	25.7	25.0	25.3	25.0	24.7	N.D.

Data from 0 to 144 hours shown in Figure 6 were detrended by sixth-order polynomials, and subjected to chi-square periodogram using Lumicycle analysis software (ActiMetrics; Wilmette, IL, USA).

Constitutively expressed MYC-BMAL1 restores circadian rhythmicity in both P_{Bmal1} and P_{Per2} activities simultaneously.

To examine whether constitutive expression of MYC-BMAL1 can restore circadian oscillation in P_{Per2} activity, I transiently introduced an Emerald Luc reporter driven by P_{Per2} (P_{Per2}::*Eluc*) into U2OS-P_{Bmal1}::*Fluc*/Δ*Bmal1*/P_{TRE3Gs}::*Myc-Bmal1* strain-2 cells, and dual-wavelength measurement of P_{Bmal1}::*Fluc* and P_{Per2}::*Eluc* was performed. Luminescence emitted from *Fluc* and *Eluc* was separated with a 600 nm long-pass filter according to the previously described method (Ono et al., 2016). The luminescence measurement in the presence of various concentrations of DOX (0, 0.01, 0.1, and 1 μg/mL) (Figure 8) showed that the addition of DOX similarly affected P_{Bmal1} and P_{Per2} activities. In the presence of DOX at 0 and 0.01 μg/mL, the intensity of luminescence from P_{Bmal1} and P_{Per2} activities unsteadily fluctuated and was weakly oscillated, while in the presence of DOX at 0.1 and 1 μg/mL, the intensity of luminescence showed clearly damped oscillation of both P_{Bmal1} and P_{Per2} activities. In the presence of DOX at 10 μg/mL, I could not obtain luminescence data possibly because simultaneous treatment with the transfection reagent and a high concentration of DOX decreased cell viability. The oscillation period of the P_{Per2} and P_{Bmal1} activities were not significantly affected by DOX concentration (Table 3). Notably, the antiphase relationship between P_{Bmal1} and P_{Per2} activities previously observed in wild-type U2OS cells was recapitulated (Ueda et al., 2005), even though the expression of functional BMAL1 was disconnected from the regulatory network of clock proteins and clock genes regulatory elements.

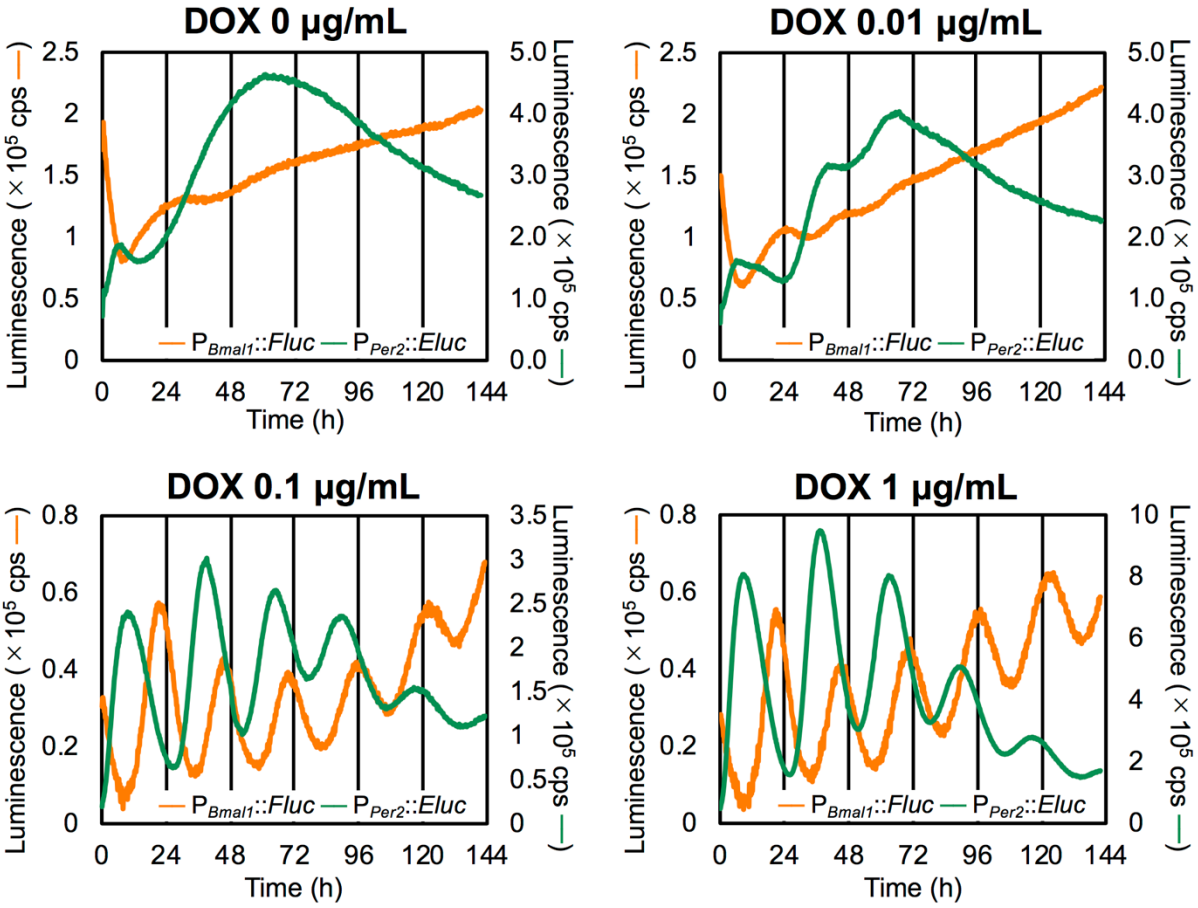

Figure 8. Constitutively expressed MYC-BMAL1 restores circadian rhythmicity in both P_{Bmal1} and P_{Per} activities. U2OS-P_{Bmal1}::*Fluc*/Δ*Bmal1*/P_{TRE3Gs}::*Myc-Bmal1* strain-2 cells were transiently transfected with the P_{Per2}::*Eluc* reporter, treated with different concentrations of doxycycline (DOX), and dual wavelength luminescence measurements of P_{Bmal1}::*Fluc* and P_{Per2}::*Eluc* were performed for 6 days. Data presented are the representative curves of three independent measurements. The orange lines show luminescence from P_{Bmal1}::*Fluc*, and the green lines show luminescence of P_{Per2}::*Eluc*.

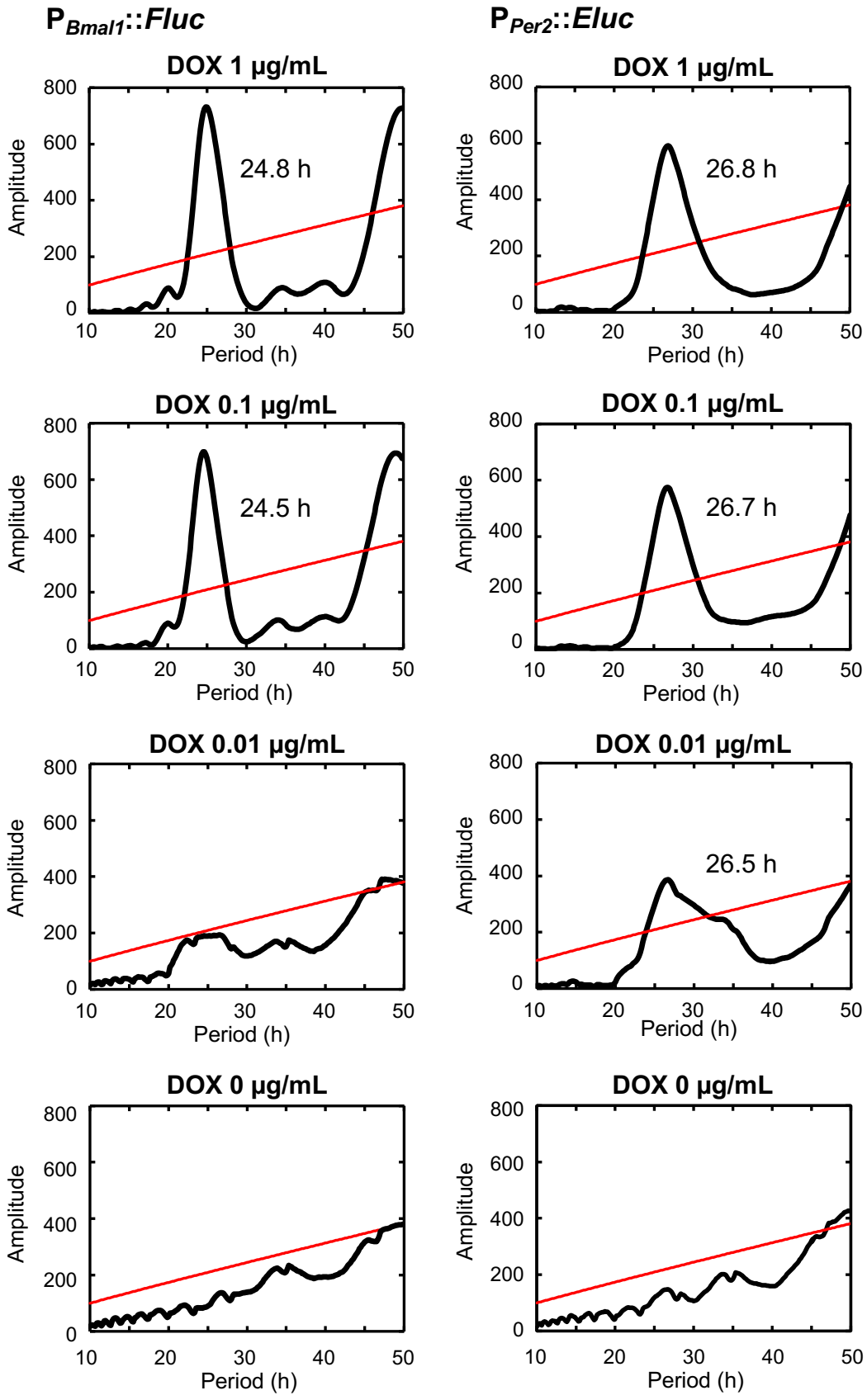
P Bmal1::Fluc
P Per2::Eluc
DOX 1 µg/mL
DOX 0.1 µg/mL
DOX 0.01 µg/mL
DOX 0 µg/mL
24.8 h
26.8 h
24.5 h
26.7 h
26.5 h
Amplitude
Period (h)
0
200
400
600
800
10
20
30
40
50

Figure 9. Periodogram analysis of P_{Bmal1}::*Fluc* and P_{Per2}::*Eluc* activities for each DOX concentration. Luminescence data from 0 to 141 hours shown in Figure 8 were subjected to chi-square periodogram analysis using Lumicycle analysis software (ActiMetrics; Wilmette, IL, USA) to assess of their oscillatory component and its significance. The black line shows the period and the red line shows the significance level ($P = 0.05$).

Table 3. Period of P_{Bmal1}::*Fluc* and P_{Per2}::*Eluc* oscillation calculated for each DOX concentration

DOX concentration (μg/mL)	1	0.1	0.01	0
Period (τ) of P_{Bmal1}::*Fluc* (h)	24.8	24.5	N.D.	N.D.
Period (τ) of P_{Per2}::*Eluc* (h)	26.8	26.7	26.5	N.D.

Data from 0 to 141 hours shown in Figure 8 were detrended by sixth-order polynomials, and subjected to chi-square periodogram using Lumicycle analysis software (ActiMetrics; Wilmette, IL, USA).

The amount of *Myc-Bmal1* mRNA did not show obvious rhythmicity in the circadian range

What makes the P_{Bmal1} activity oscillate? In general, even though the rate of transcription and translation is constant, rhythmicity in mRNA and protein abundance can be generated by rhythmicity in their half-life (Lück et al., 2014), which can induce rhythmicity in P_{Bmal1} activity. Therefore, it is possible that the amount of *Myc-Bmal1* mRNA and protein exhibit circadian rhythm even though it is driven by a constitutive promoter. To confirm this point, I performed quantitative RT-PCR and immunoblot analyses.

The amount of mRNA coding MYC-BMAL1 from 24 to 52 hours after DOX addition at various concentrations (0, 0.01, 0.1, 1 and 10 μg/mL) was measured by quantitative RT-PCR. The average levels of *Myc-Bmal1* mRNA from 24 to 52 hours increased in accordance with the DOX concentration, it increased strikingly between DOX 0.01 and 0.1 μg/mL (Figure 10A), the same concentration range where both the oscillation's robustness and baseline stability were improved remarkably (Figure 6). No obvious circadian rhythmicity in *Myc-Bmal1* mRNA levels was observed in the presence of DOX from 0 to 10 μg/mL (Figure 10, B-F), while endogenous *Bmal1* transcript from wild-type U2OS-P_{Bmal1}::*Fluc* cells showed clear oscillation (Figure 10G) with its peak and trough coinciding with those of P_{Bmal1} activity (Figure 6, see the WT trace). For *Myc-Bmal1* mRNA, no such association was found in the presence of DOX at various concentrations. From these results, it is unlikely that oscillation in P_{Bmal1} activity is driven by rhythmic accumulation of transcriptional products of the gene coding MYC-BMAL1.

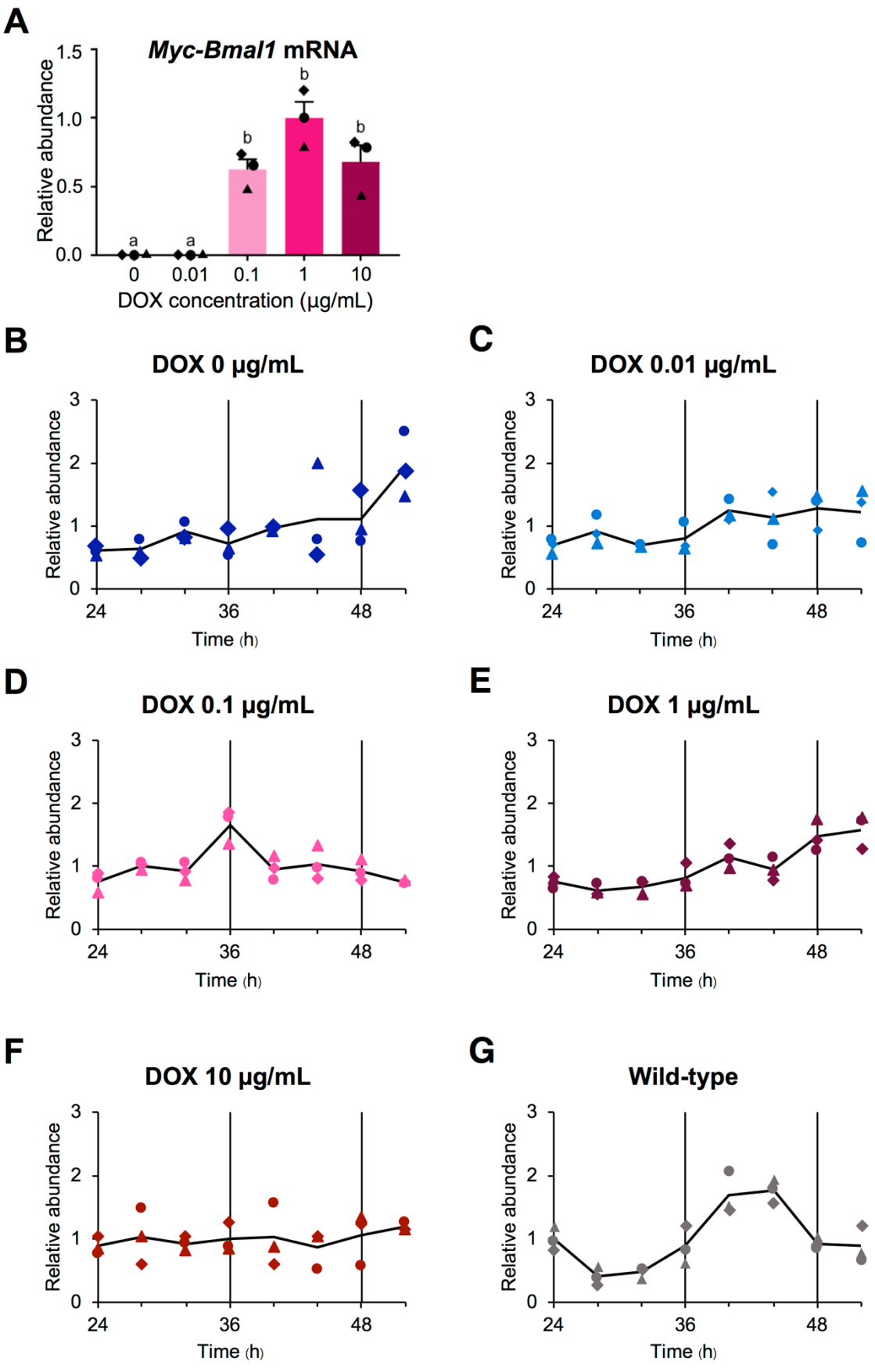
A
Myc-Bmal1 mRNA
Relative abundance
1.5
1.0
0.5
0.0
a
a
b
b
b
0
0.01
0.1
1
10
DOX concentration (μg/mL)
B
DOX 0 μg/mL
C
DOX 0.01 μg/mL
D
DOX 0.1 μg/mL
E
DOX 1 μg/mL
F
DOX 10 μg/mL
G
Wild-type
Relative abundance
Time (h)
24
36
48
0
1
2
3

Figure 10. *Myc-Bmal1* mRNA accumulation did not show significant circadian rhythmicity. Total RNA samples were collected from U2OS-P_{Bmal1}::*Fluc*/Δ*Bmal1*/P_{TRE3Gs}::*Myc-Bmal1* strain-2 cells cultured every 4 hours from 24 to 52 hours after the addition of 100 nM of dexamethasone (time 0). (A) Graphs showing relative *Myc-Bmal1* mRNA accumulations after treatment with different concentrations of doxycycline (DOX) in the presence of DOX at 0, 0.01, 0.1, 1, and 10 μg/mL. For *Myc-Bmal1* mRNA accumulations, the average of all the time-points analyzed in each DOX concentration was calculated. Results were normalized using the average values of DOX at 1 μg/mL, and data are shown as the mean ± SEM. N = 3 samples/group, one-way ANOVA followed by Tukey's multiple comparison tests, different characters (a and b) indicate significant differences ($P < 0.05$). (B-F) Time curve of *Myc-Bmal1* mRNA expression after addition of dexamethasone (time 0) in the presence of DOX at 0 μg/mL (B), 0.01 μg/mL (C), 0.1 μg/mL (D), 1 μg/mL (E), 10 μg/mL (F) and endogenous *Bmal1* mRNA from wild-type U2OS-P_{Bmal1}::*Fluc* (G). Total RNA samples were subjected to quantitative reverse-transcription PCR analysis. Relative expression was calculated using Pfaffl's method (Pfaffl, 2001) with *GAPDH* as an internal control. Markers (▲,◆, and ●) indicate three biological replicates. Values were normalized against the average of all time points in each series. Lines in black indicate the average values of the three biological replicates.

The amount of MYC-BMAL1 protein did not show obvious rhythmicity in the circadian range

For immunoblot analysis, I prepared the time series samples of total protein from U2OS-P$_{Bmal1}$::*Fluc*/Δ*Bmal1*/P$_{TRE3Gs}$::*Myc-Bmal1* strain-2 cells every 4 hours from 0 to 52 hours after the addition of 100 nM of dexamethasone and subjected to immunoblot analysis using an anti-Myc antibody.

To examine DOX-induced changes in the overall levels of MYC-BMAL1 protein, equal volume mixtures of samples from 0 to 52 hours after stimulation in the presence of various DOX concentrations were analyzed (Figure 11, Table 4). The levels of MYC-BMAL1 protein increased in accordance with the DOX concentration. As is the case for *Myc-Bmal1* mRNA, the amount of MYC-BMAL1 protein increased remarkably between DOX at 0.01 and 0.1 μg/mL (Figure 11A), suggesting that there is a threshold value of MYC-BMAL1 protein amount that can induce clear circadian oscillation.

Then, I assessed the time-course changes in the accumulation levels of MYC-BMAL1 protein in the presence of DOX at 0, 0.01, 0.1, 1, and 10 μg/mL (Figure 11, B-F). To test whether MYC-BMAL1 protein levels change in a circadian manner, statistical analysis was performed using JTK cycle test (Hughes et al., 2010). It is a non-parametric test method that analyzes discrete time-series data with a relatively small number of data points for statistically significant rhythmicity. It provides permutation-based *P*-values (ADJ.*P*), as well as optimum phase (LAG), amplitude, and period estimations for each transcript (Table 4) (Hughes et al., 2010). While the luminescence traces from P$_{Bmal1}$::*Fluc* (Figure 6) showed robust rhythmicity in the presence of DOX at 0.1 and 1 μg/mL, no significant rhythmicity within the circadian range (between 20 and 28 hours) was detected in MYC-BMAL1 protein accumulation at any concentrations of DOX (JTK cycle test, ADJ.$P > 0.05$) (Table 4).

Next, I examined the time-course of changes in the accumulation of endogenous BMAL1 in wild-type U2OS-P$_{Bmal1}$::*Fluc* using an anti-ARNTL (BMAL1) antibody (Figure 11G). In contrast to the accumulation of endogenous *Bmal1* mRNA, no significant rhythmicity was observed at the protein levels. Of note, multiple bands were detected for endogenous BMAL1, possibly representing phosphorylated forms (Yoshitane et al., 2009), which were not prominent in DOX-induced MYC-BMAL1.

I also compared the average levels of DOX-induced MYC-BMAL1 protein levels in strain-2 cells collected from 0 to 52 hours every 4 hours interval with that of endogenous BMAL1 expressed in wild-type U2OS cells (Figure 12). The amount of endogenous BMAL1 was about 25% of that of MYC-BMAL1 induced in the presence of DOX at 1 μg/mL. These findings suggested the biological significance of rhythmic promoters suggesting that increased BMAL1 expression is required when it is driven by a non-rhythmic promoter.

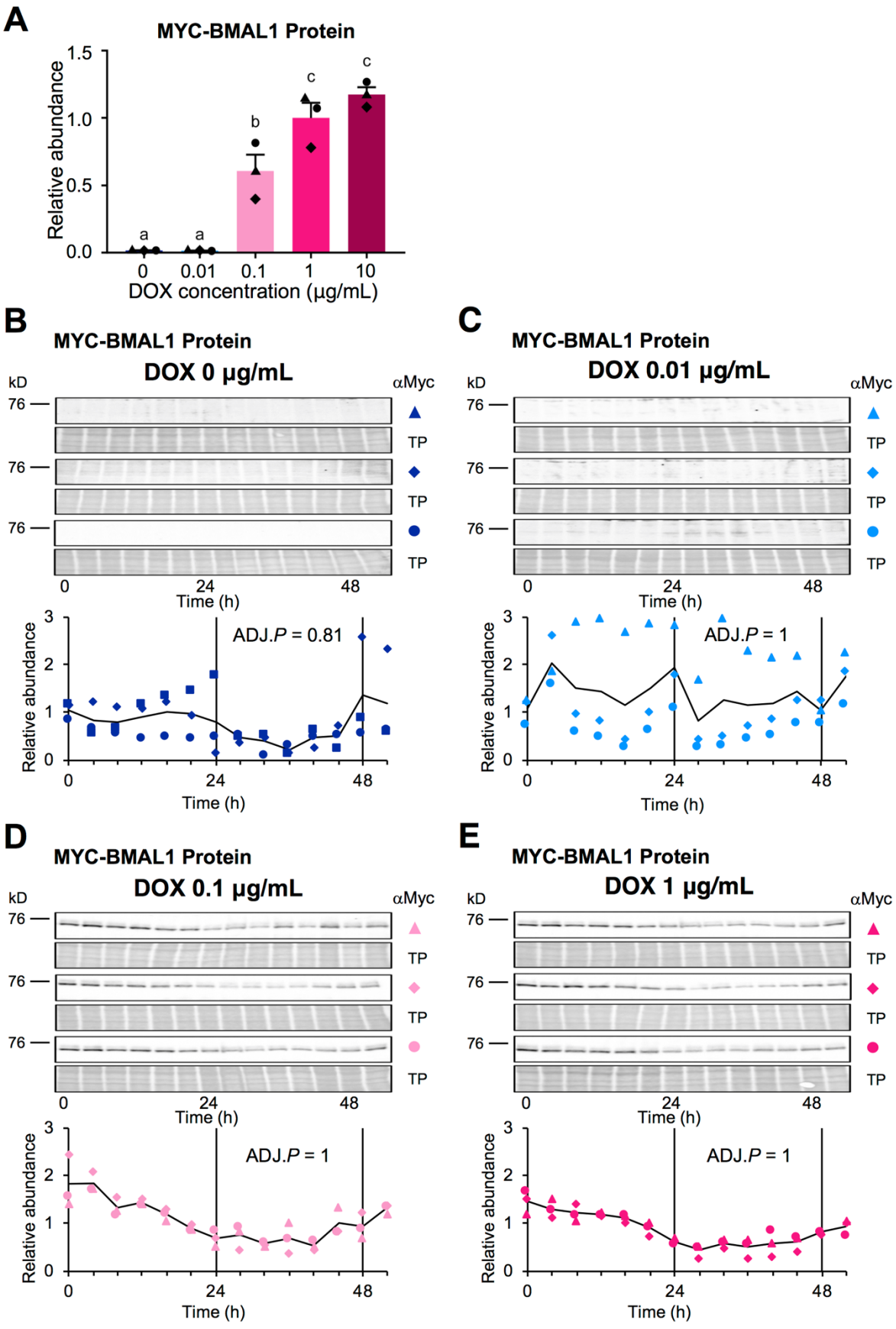
A
MYC-BMAL1 Protein
Relative abundance
1.5
1.0
0.5
0.0
a
a
b
c
c
0
0.01
0.1
1
10
DOX concentration (μg/mL)
B
MYC-BMAL1 Protein
DOX 0 μg/mL
kD
αMyc
76
TP
Time (h)
0
24
48
Relative abundance
ADJ.P = 0.81
C
MYC-BMAL1 Protein
DOX 0.01 μg/mL
ADJ.P = 1
D
MYC-BMAL1 Protein
DOX 0.1 μg/mL
ADJ.P = 1
E
MYC-BMAL1 Protein
DOX 1 μg/mL
ADJ.P = 1

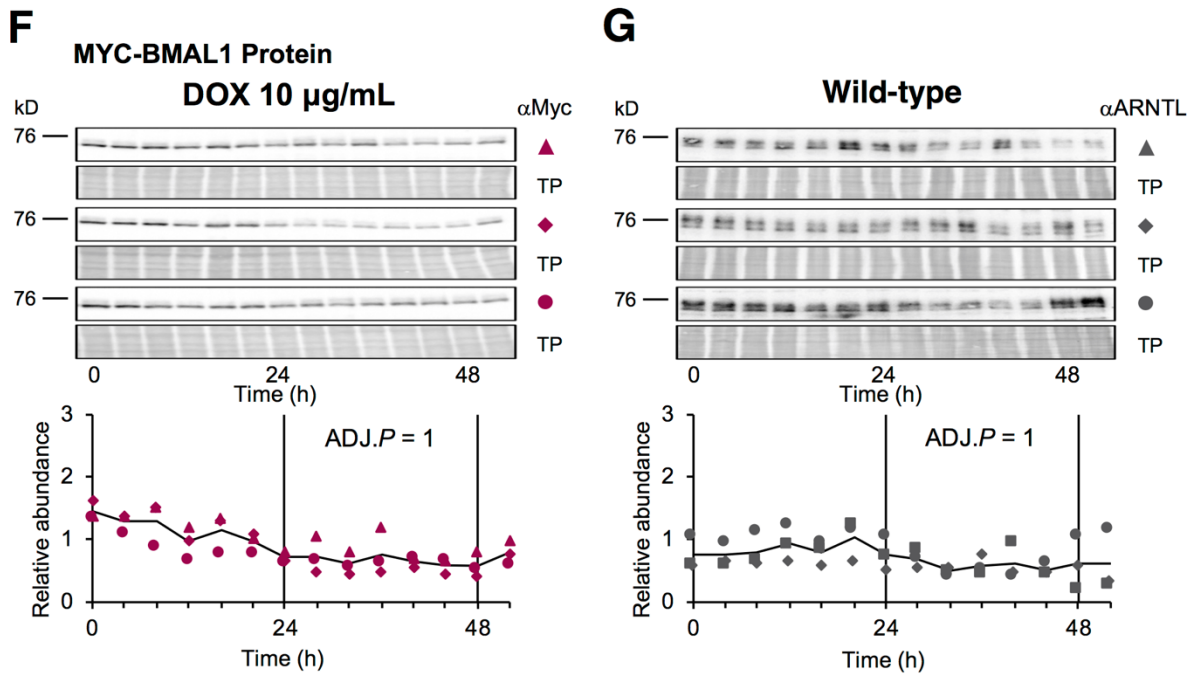

Figure 11. MYC-BMAL1 protein did not show significant circadian rhythmicity. Total protein samples were collected from U2OS-P$_{Bmal1}$::*Fluc*/Δ*Bmal1*/P$_{TRE3Gs}$::*Myc-Bmal1* strain-2 cells cultured every 4 hours from 24 to 52 hours after the addition of 100 nM of dexamethasone (time 0). (A) Graphs showing the relative amount of MYC-BMAL1 protein after treatment with different concentrations of doxycycline (DOX). For protein accumulation, equal amounts of the protein samples collected within each DOX concentration were mixed and subjected to immunoblot analysis using an anti-Myc antibody. Results were normalized using the average value of DOX at 1 µg/mL, and data are shown as the mean ± SEM. N = 3 samples/group, one-way ANOVA followed by Tukey's multiple comparison test, different characters (a, b, c) indicate significant differences (P < 0.05). (B-G) Time curve of MYC-BMAL1 protein expression after addition of dexamethasone (time 0) in the presence of DOX at 0 µg/mL (B), 0.01 µg/mL (C), 0.1 µg/mL (D), 1 µg/mL (E), 10 µg/mL (F) and from wild-type U2OS cells (G). Protein samples were collected and subjected to immunoblot analysis in three independent experiments. Markers (▲,◆, and ●) indicate MYC-BMAL1 bands in three biological replicates, and TP indicates total protein stains (upper panels). Graphs show the quantification

of MYC-BMAL1 protein amount by densitometry (lower panels). The intensity of each band was normalized by total protein, and values were normalized against the mixture of the samples of all time points in each series. Lines in black indicate the average values of the three biological replicates. No significant rhythmicity in the circadian range (between 20 to 28 hours) was detected in the presence of DOX at 0, 0.01, 0.1, 1, and 10 μg/mL (JTK cycle test, ADJ.*P* = 0.81 in the presence of DOX at 0 μg/mL and ADJ.*P* = 1 in the presence of DOX from 0.01 to 10 μg/mL and in wild-type U2OS cells).

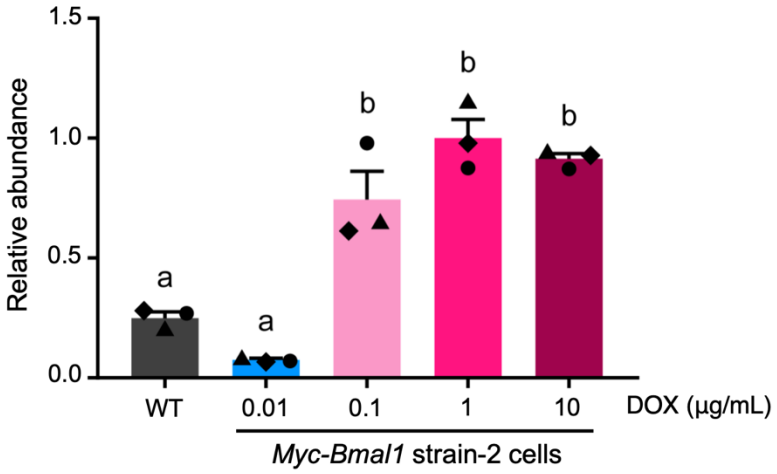

Figure 12. MYC-BMAL1 protein levels of U2OS-P$_{Bmal1}$::*Fluc*/Δ*Bmal1*/P$_{TRE3Gs}$::*Myc-Bmal1* strain-2 cells. Total protein samples were collected from U2OS-P$_{Bmal1}$::*Fluc*/Δ*Bmal1*/P$_{TRE3Gs}$::*Myc-Bmal1* strain-2 cells cultured every 4 hours from 24 to 52 hours after the addition of 100 nM of dexamethasone (time 0) and mixed the cell lysate from 24 to 52 hours before SDS-PAGE. Graphs showing the relative amount of MYC-BMAL1 protein after treatment with different concentrations of doxycycline (DOX). For protein accumulation, equal amounts of the protein samples collected within each DOX concentration were mixed and subjected to immunoblot analysis using an anti-Myc antibody for *Myc-Bmal1* strain-2 cells and using an anti-ARNTL antibody for wild-type U2OS cells. Results were normalized using the average value of DOX at 1 μg/mL, and data are shown as the mean ± SEM. N = 3 samples/group, one-way ANOVA followed by Tukey's multiple comparison test, different characters (a, b) indicate significant differences ($P < 0.05$). Protein samples were collected and subjected to immunoblot analysis in three independent experiments. Markers (▲,◆, and ●) indicate MYC-BMAL1 in three biological replicates.

The amount of the proteins involved in ROR/REV/Bmal1 loop did not show obvious rhythmicity in the circadian range

In the current mammalian TTFL model, BMAL1, CLOCK, REV-ERBs and RORs constitute ROR/REV/*Bmal1* loop (Cho et al., 2012; Sato et al., 2004; Preitner et al., 2002). REB-ERBs and RORs positively and negatively regulate *Bmal1* transcription, respectively, and compete for RORE located in the upstream region of *Bmal1*, resulting in circadian oscillation in *Bmal1* transcription (Guillaumond et al., 2005). CLOCK-BMAL1 heterodimer positively regulates the transcription of REB-ERBs and RORs.

It is possible that REB-ERBs and/or RORs accumulate in a circadian manner to generate circadian oscillation in P_{Bmal1} activity. To test this possibility, I measured the levels of REV-ERBα protein by immunoblot analysis. To examine DOX-induced changes at the overall levels of REV-ERBα protein, an equal volume mixture of samples from 0 to 52 hours was analyzed (Figure 13, Table 4). The levels of REV-ERBα protein exhibited an ascending trend as the DOX concentration increased (Figure 13A). However, in contrast to MYC-BMAL1 protein expression levels (Fig. 11A), no significant change was observed between DOX at 0.01 and 0.1 μg/mL. Then, I assessed the time-course of changes at the accumulation levels of REV-ERBα in the presence of DOX at 0, 0.01, 0.1, 1, and 10 μg/mL (Figure 13, B-F) No significant rhythmicity within the circadian range (between 20 and 28 hours) was detected at any concentrations of DOX (JTK cycle test, ADJ.P > 0.05) (Table 4) (Hughes et al., 2010). I also examined the time-course changes in the accumulation of endogenous BMAL1 in wild-type U2OS-P_{Bmal1}::*Fluc* using an anti-REV-ERBα antibody (Figure 13G), significant rhythmicity was observed in the protein levels (ADJ.P = 3.904×10^{-6}). I also tried to examine the DOX-induced changes in the overall levels of RORα protein, and the time-course changes in the accumulation levels of RORα protein in the presence of DOX at 0.1 and 1 μg/mL, however, I could not obtain data because the reactivity of the antibody was not satisfactory.

According to the current model, CLOCK-BMAL1 activates the transcription of REV-ERBs and RORs. To examine DOX-induced changes at the overall levels of CLOCK protein, an equal volume mixture of samples from 0 to 52 hours after the stimulation was analyzed (Figure 14, Table 4). The average levels of CLOCK protein in the presence of DOX at 0.1 μg/mL was approximately five-fold higher than that of DOX at 0.01 μg/mL (Figure 14A). Then, I assessed the time-course changes in the accumulation levels of CLOCK protein in the presence of DOX at 0.1 and 1 μg/mL (Figure 14, B-C). In the presence of DOX at 0.1 μg/mL, no significant rhythmicity within the circadian range (between 20 and 28 hours) was detected for CLOCK protein accumulation (JTK cycle test, ADJ.P > 0.05) (Table 4) (Hughes et al., 2010). In the presence of DOX at 1 μg/mL it showed significant rhythmicity (JTK cycle test, ADJ.P < 0.05), although the amplitude value was calculated to be 0.229 for CLOCK protein in the presence of DOX at 1 μg/mL using JTK cycle test (Table 4), suggesting that the rhythmicity of CLOCK protein accumulation, if any, was very weak. This weak oscillation seems not functional because any circadian oscillation was not detected in the levels of REV-ERBα protein. From the data shown in Figure 13 and Figure 14, it is not likely that the oscillation in P_{Bmal1} activity is driven by the oscillation in the levels of ROR/REV/Bmal1 loop component proteins.

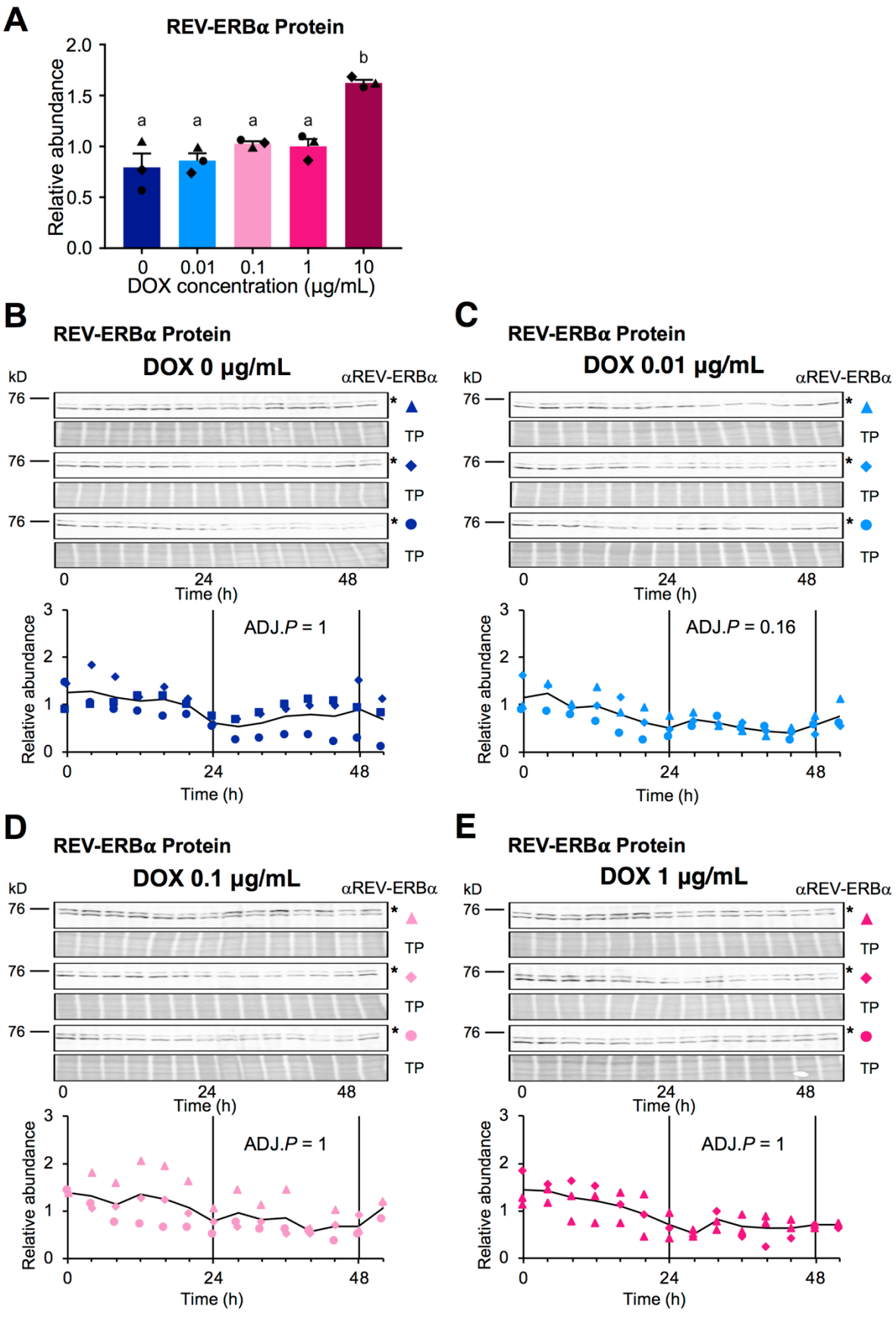
A
REV-ERBα Protein
Relative abundance
2.0
1.5
1.0
0.5
0.0
a
a
a
a
b
0
0.01
0.1
1
10
DOX concentration (μg/mL)
B
REV-ERBα Protein
DOX 0 μg/mL
kD
αREV-ERBα
76
TP
Time (h)
ADJ.P = 1
Relative abundance
C
REV-ERBα Protein
DOX 0.01 μg/mL
ADJ.P = 0.16
D
REV-ERBα Protein
DOX 0.1 μg/mL
ADJ.P = 1
E
REV-ERBα Protein
DOX 1 μg/mL
ADJ.P = 1

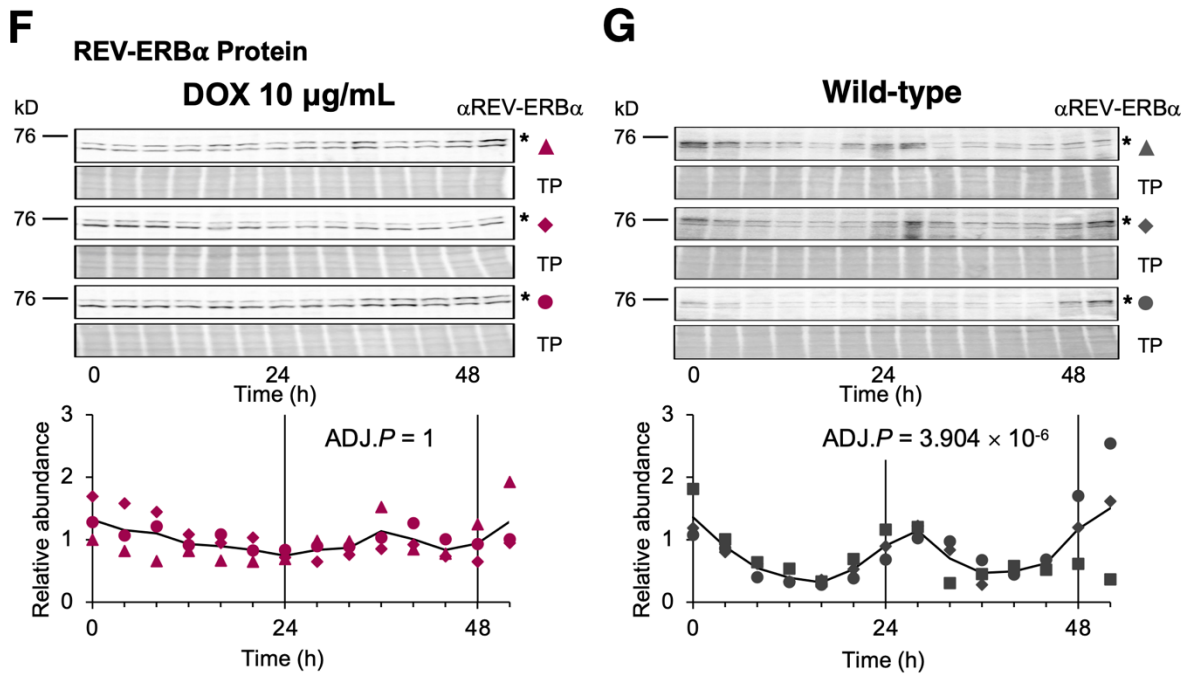

Figure 13. REV-ERBα protein did not show significant circadian rhythmicity. Total protein samples were collected from U2OS-P$_{Bmal1}$::*Fluc*/Δ*Bmal1*/P$_{TRE3Gs}$::*Myc-Bmal1* strain-2 cells cultured every 4 hours from 24 to 52 hours after addition of 100 nM of dexamethasone (time 0). (A) Graphs showing relative REV-ERBα protein after treatment with different concentrations of doxycycline (DOX). For protein accumulation, equal amounts of the protein samples collected within each DOX concentration were mixed and subjected to immunoblot analysis using anti-REV-ERBα antibody. Results were normalized using the average values of DOX at 1 μg/mL, and data are shown as the mean ± SEM. N = 3 samples/group, one-way ANOVA followed by Tukey's multiple comparison test, different characters (a and b) indicate significant differences ($P < 0.05$). (B-G) Time curve of REV-ERBα protein expression after addition of dexamethasone (time 0) in the presence of DOX at 0 μg/mL (B), 0.01 μg/mL (C), 0.1 μg/mL (D), 1 μg/mL (E), 10 μg/mL (F), and from wild-type U2OS cells (G). Protein samples were collected and subjected to immunoblot analysis in three independent experiments. Markers (▲,◆, and ●) indicate REV-ERBα bands in three biological replicates, and TP indicates total protein stains. Asterisks in B-G indicate nonspecific bands (upper panels). Graphs (lower panels) show the quantification of REV-ERBα protein amount by densitometry.

The intensity of each band was normalized by total protein, and values were normalized against the mixture of the samples of all time points in each series. Lines in black indicate the average values of the three biological replicates. No significant rhythmicity in the circadian range (between 20 to 28 hours) was detected in the presence of DOX at 0, 0.01, 0.1, 1, and 10 μg/mL (JTK cycle test, ADJ.P = 0.16 in the presence of DOX at 0.01 μg/mL and ADJ.P = 1 in the presence of DOX at 0, 0.1, 1, and 10 μg/mL). Significant rhythmicity in wild-type U2OS cells (ADJ.P = 3.904×10^{-6}).

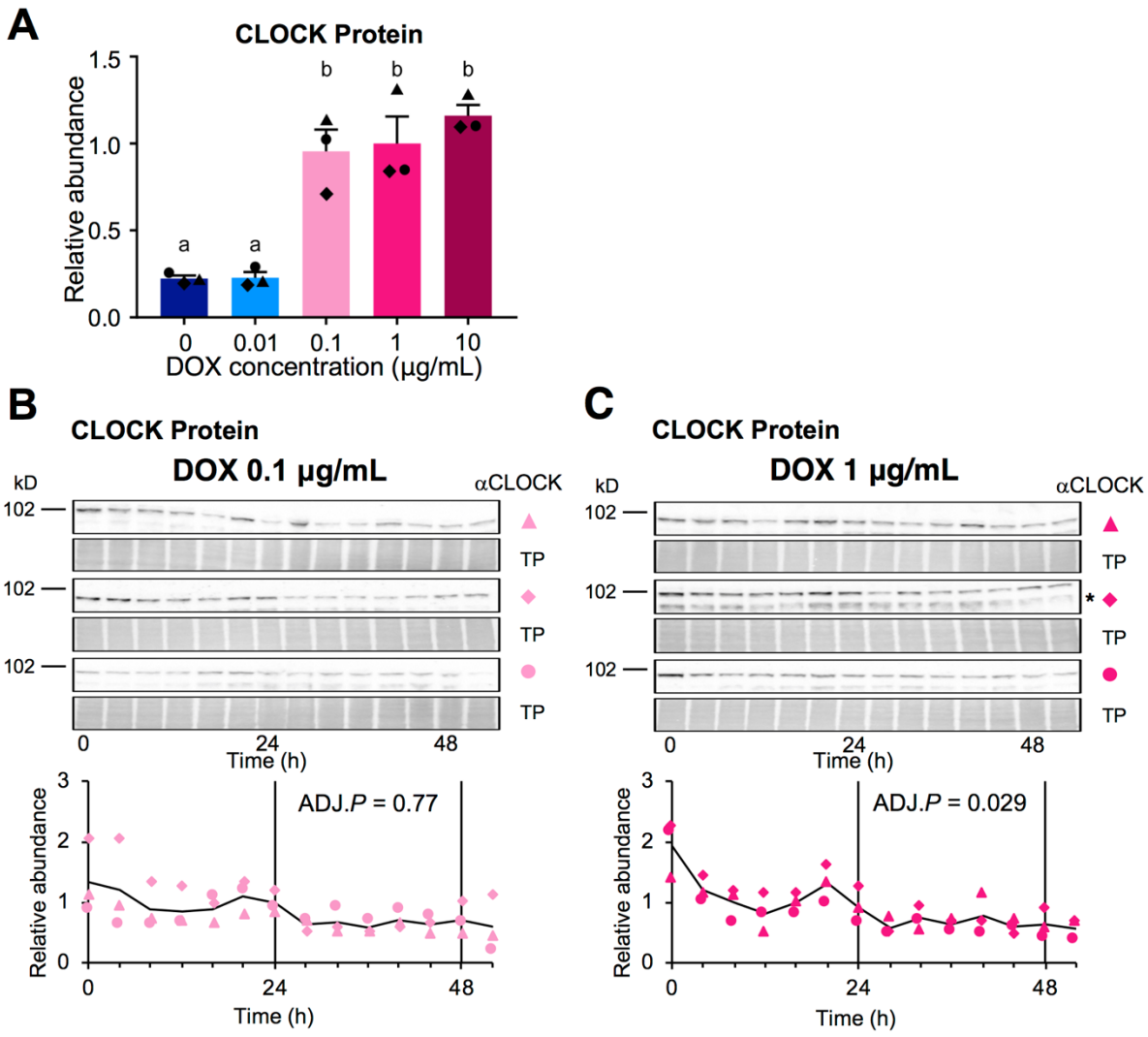

Figure 14. CLOCK protein did not show clear circadian rhythmicity. Total protein samples were collected from U2OS-P$_{Bmal1}$::*Fluc*/Δ*Bmal1*/P$_{TRE3Gs}$::*Myc-Bmal1* strain-2 cells cultures every 4 hours from 24 to 52 hours after the addition of 100 nM of dexamethasone (time 0). (A) Graphs showing relative CLOCK protein after treatment with different concentrations of doxycycline (DOX). For protein accumulation, equal amounts of the protein samples collected within each DOX concentration were mixed and subjected to immunoblot analysis using anti-CLOCK antibody. Results were normalized using the average values of DOX at 1 μg/mL and data are shown as the mean ± SEM. N = 3 samples/group, one-way ANOVA followed by Tukey's multiple comparison test, different characters (a and b) indicate significant differences ($P < 0.05$). (B-F) Time curve of CLOCK protein expression after

addition of dexamethasone (time 0) in the presence of DOX at 0.1 μg/mL (B) and 1 μg/mL (C). Protein samples were collected and subjected to immunoblot analysis in three independent experiments (upper panels). Markers (▲,◆, and ●) indicate CLOCK bands in three biological replicates, and TP indicates total protein stains. Asterisks in C indicate nonspecific bands. Graphs (lower panels) show the quantification of CLOCK protein amount by densitometry. The intensity of each band was normalized by total protein, and values were normalized against the mixture of the samples of all time points in each series. Lines in black indicate the average values of the three biological replicates. No significant rhythmicity in the circadian range (between 20 to 28 hours) was detected in the presence of DOX at 0.1 and 1 μg/mL (JTK cycle test, ADJ.*P* = 0.77). In the presence of DOX at 1 μg/mL, significant circadian rhythmicity with a period of 20 hours and an amplitude of 0.229 was observed (ADJ.*P* = 0.029, see also Table 4).

Table 4. JTK cycle test of U2OS-P$_{Bmal1}$::*Fluc*/Δ*Bmal1*/P$_{TRE3Gs}$::*Myc-Bmal1* strain-2 cells at each DOX concentration

JTK cycle test	ADJ.*P*	Period	LAG	Amplitude
MYC-BMAL1				
DOX 0 μg/mL	0.81	24	2	0.079
DOX 0.01 μg/mL	1	20	2	0.377
DOX 0.1 μg/mL	1	24	0	0.136
DOX 1 μg/mL	1	20	2	0.13
DOX 10 μg/mL	1	28	4	0.167
Wild-type	1	20	4	0.077
REV-ERBα				
DOX 0 μg/mL	1	20	18	0.111
DOX 0.01 μg/mL	0.16	28	4	0.147
DOX 0.1 μg/mL	1	28	4	0.133
DOX 1 μg/mL	1	28	6	0.13
DOX 10 μg/mL	1	28	6	0.095
Wild-type	3.904×10^{-6}	28	0	0.348
CLOCK				
DOX 0.1 μg/mL	0.77	20	2	0.234
DOX 1 μg/mL	0.029	20	0	0.229

Transient response analysis of the P_{Bmal1} activity

The most widely applicable technique for analyzing forced dynamic response is transient response analysis. Its goal is to find out a transfer function expressing how a system responds to input stimulation, *i.e.*, an input-output relationship (Golnaraghi and Kuo, 2009; Ogata, 2010). In this analysis, a function in the time domain (t-domain) that specifically expresses the time-dependent behavior of a system (e.g. luminescence from P_{Bmal1}::*Fluc*) is converted into that in the frequency domain (s-domain) by the Laplace transform. The Laplace transform converts the differential equations in the t-domain into algebraic equations in the s-domain, which makes solving differential equations to be easier. Conversely, s-domain functions can be converted to t-domain functions by inverse Laplace transform.

I subjected the time-course data of P_{Bmal1}::*Fluc* luminescence to transient response analysis to find out the mechanism underlying the generation of circadian oscillations under constitutive MYC-BMAL1 expression. In this framework, the administration of dexamethasone was considered as the input to stimulate P_{Bmal1} activity. The transfer functions were estimated using the System Identification Toolbox pre-installed in MATLAB (version R2019b; MathWorks, Natick, MA).

A unit step input into the system was used to approximate the administration of 100 nM of dexamethasone at time 0, which can be expressed by the following unit step function:

$$u(t) = \begin{cases} 0 \ (t < 0) \\ 1 \ (t \geq 0) \end{cases} \qquad (1).$$

Denoting $U(s)$ and $Y(s)$ as the Laplace transforms of the input and output signals, respectively, the transfer function $G(s)$ is represented as:

$$G(s) = \frac{Y(s)}{U(s)} \qquad (2).$$

P_{Bmal1} activity in the presence of DOX at 1 μg/mL was approximated by the following transfer function, with two poles and no zeros (Figure 15, DOX 1 μg/mL):

$$G(s) = \frac{b_0}{s^2+a_1 s+a_0} \qquad (3).$$

The coefficients were estimated as $a_1 = 0.03214$, $a_0 = 0.06171$, $b_0 = 34.42$. This formula can be rewritten as the following second-order system representing a damped oscillator:

$$G(s) = K \cdot \frac{{\omega_n}^2}{s^2+2\zeta\omega_n s+{\omega_n}^2} \qquad (4).$$

where ω_n, is the natural angular velocity, a frequency or rate at which an object naturally vibrates, ζ is the damping coefficient, an influence on an oscillatory system that lessens or stops it from oscillating, and *K* is the gain, the relationship between the input to the output signal at a steady state; when the baseline increase, gain parameter show very high value (Marghitu et al., 2001). Using ω_n and ζ, the period τ of the damped oscillator is determined as

$$\tau = \frac{2\pi}{w_n\sqrt{1-\zeta^2}} \qquad (5).$$

On the other hand, P_{Bmal1} activity in the presence of DOX at 0.05 and 0.1 μg/mL were approximated by the following third-order transfer function with three poles and no zeros (Figure 15, DOX 0.05 and 0.1 μg/mL):

$$G(s) = \frac{b_0}{(s^2+a_1 s+a_0)(c_0 s+1)} \qquad (6).$$

The coefficients were estimated as $a_1 = 0.02363$, $a_0 = 0.06411$, $b_0 = 224.6$, $c_0 = 118.4$ for DOX 0.05 μg/mL; and $a_1 = 0.01804$, $a_0 = 0.06051$, $b_0 = 75.58$, $c_0 = 350.2$ for DOX 0.1 μg/mL. This third-order transfer function can be decomposed into first-order and second-order systems as follows:

$$G(s) = K \cdot \frac{1}{T_s s+1} \cdot \frac{{\omega_n}^2}{s^2+2\zeta\omega_n s+{\omega_n}^2} \qquad (7).$$

In the first-order system (*i.e.*, $\frac{1}{T_s s+1}$), the time constant T_s characterizes the response time required for the baseline of the luminescence signal to rise exponentially to its steady state. The values of parameters calculated for each DOX concentration are listed in Table 5. This analysis indicated that in the presence of DOX at 0.01 μg/mL, the P_{Bmal1} activity was

approximated using the following six-order transfer function with six poles and six zeros as follows:

$$G(s) = \frac{4756s^6+431.4s^5+276s^4+14.22s^3+3.075s^2+0.04085s+0.006588}{s^6+0.3191s^5+0.06675s^4+0.01035s^3+0.0006645s^2+3.197e^{-5}s+1.083e^{-6}}$$

A higher-order transfer function was required to describe the behavior of P_{Bmal1} activity, which is difficult to interpret using a combination of basic elements (Figure 15, DOX 0.01 μg/mL). It is possible that baseline P_{Bmal1} activity became uncontrollable when the MYC-BMAL1 concentration was too low.

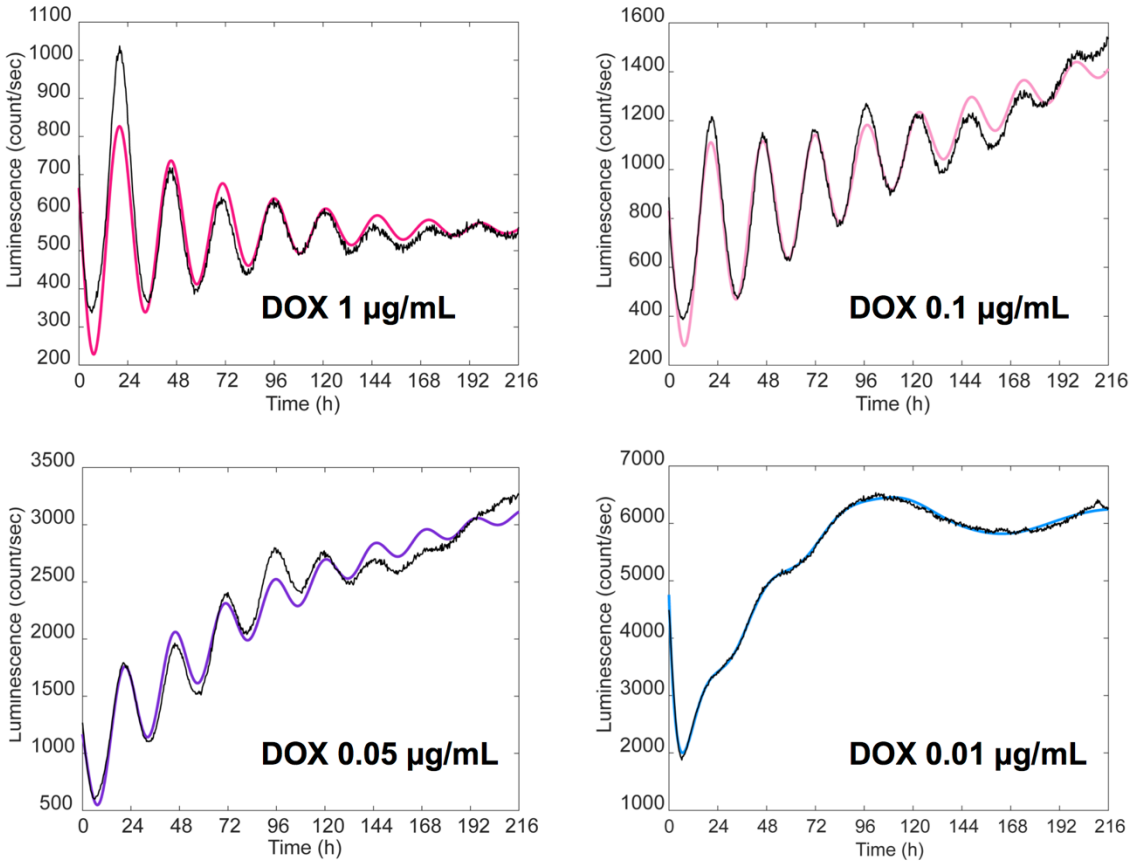

Figure 15. Transfer functions reproducing the behaviors of P_{Bmal1} activity obtained by transient response analysis. Luminescence data of P_{Bmal1} activity in the presence of doxycycline (DOX) at 1, 0.1, 0.05, and 0.01 μg/mL shown in Figure 6 were subjected to transient response analysis. Experimental values of luminescence intensity are shown in black and simulated data (inverse Laplace transform of $G(s) \cdot U(s)$) are shown in red for DOX 1 μg/mL (upper left panel), pink for DOX 0.1 μg/mL (upper right panel), purple for DOX 0.05 μg/mL (bottom left panel), and blue for DOX 0.01 μg/mL (bottom right panel).

Table 5. Parameters of oscillation calculated for each DOX concentration

DOX concentration (μg/mL)	1	0.1	0.05
Natural angular velocity (ω_n) (h^{-1})	0.2484	0.2460	0.2532
Damping coefficient (ζ) (h^{-1})	0.06469	0.03668	0.04667
*Period (τ) (h)	25.4	25.6	24.8
Time constant (T_s) (h^{-1})	–	350.2	118.4
Gain (K)	557.8	1249	3504

*Calculated by substituting ω_n and ζ values into Equation 5.

Discussion

Circadian rhythms are biological oscillations caused by an endogenous timing system that regulates activities such as sleep/wake cycles, metabolic balance, and hormone production oscillating with a period length of approximately 24 hours (Rijio and Takahashi, 2019; Takahashi., 2017). The current molecular mechanism for understanding circadian oscillations in the transcription of clock genes has been TTFL (Takahashi., 2017) (Figure 1). However, this TTFL model cannot fully explain why the constitutive expression of clock genes can restore circadian oscillations. In this study, I performed quantitative experiments by establishing a novel P_{Bmal1}::*Fluc* reporter cell line in which endogenous *Bmal1* is inactivated by CRISPR-Cas9 and exogenous *Bmal1* is expressed under a DOX-inducible promoter (Figure 3).

The results of this study demonstrate that DOX concentrations had a significant impact on the luminescence of the P_{Bmal1}::*Fluc* reporter (Figure 6). In particular, in the presence of DOX from 0.2 to 1 μg/mL, P_{Bmal1} activity showed damped oscillation with gradual stabilization at a value specific to each DOX concentration. Moreover, circadian oscillation in P_{Per2} activity can also be restored by constitutive expression of MYC-BMAL1 (Figure 8). In the presence of DOX at 0.1 and 1 μg/mL. In the P_{Per2} activity showed luminescence activity clearly antiphase with P_{Bmal1} activity as in wild-type U2OS cells. I further tested the levels of exogenous *Bmal1* in the presence of various concentrations of DOX using quantitative RT-PCR from 24 to 52 hours (Figure 10) and immunoblotting from 0 to 52 hours (Figure 11). No significant circadian rhythmicity was observed for the transcriptional and translational products in the presence of DOX from 0 to 10 μg/mL.

I tested whether the accumulation of proteins involved in the ROR/REV/*Bmal1* loop exhibited circadian rhythmicity. The accumulation levels of REV-ERBα protein (Figure 13) in the presence of DOX at 0.1 and 1 μg/mL, and that of CLOCK protein levels in the presence of

DOX at 0.1 μg/mL (Figure 14) did not show significant circadian rhythmicity by JTK cycle test.

The accumulation of CLOCK protein in the presence of DOX at 1 μg/mL (Figure 14C) showed significant but quite weak rhythmicity with an amplitude value of 0.229. For the following reasons, I anticipate that this CLOCK rhythmicity is not the factor underlying the P_{Bmal1} oscillation. No studies have been reported proving that CLOCK directly binds to the regulatory region of *Bmal1* to regulate transcription. The CLOCK-BMAL1 heterodimer controls the expression of REV-ERBs and RORs, whose translational products bind to the regulatory region of *Bmal1* to regulate transcription. However, as shown in Figure 11, the REV-ERBα protein show no significant rhythmicity in the presence of DOX at 0.1 and 1 μg/mL while it shows clear circadian rhythmicity in wild-type U2OS cells (Figure 13G). Therefore, it is unlikely that robust circadian oscillations of the P_{Bmal1} and P_{Per2} activity levels are driven by oscillations at the protein levels, although this possibility cannot be completely ruled out.

BMAL1, CLOCK, and REV-ERBs exhibit circadian oscillations in their phosphorylation state (Robles et al., 2017; Lee et al., 2001). More specifically, circadian oscillations in the phosphorylation of CLOCK and BMAL1 are thought to be crucial in regulating subcellular localization, stability, protein-protein interactions, and transcriptional activity (Tamaru et al., 2009; Yoshitane et al., 2009). Detection of the electrophoretic mobility change of the bands during SDS-PAGE is a common method for identifying phosphorylated proteins (Lee et al., 2019). However, I was unable to identify notable band shifts of BMAL1, REV-ERBα, and CLOCK proteins that exhibit circadian rhythm (Figures 11, 13, and 14) and the time-course changes in the accumulation of endogenous BMAL1 in wild-type U2OS-P_{Bmal1}::*Fluc*. It should be underlined that endogenous BMAL1 was found as multiple bands, possibly in phosphorylated forms (Yoshitane et al., 2009), which were not prominent in DOX-induced MYC-BMAL1. Therefore, it seems unlikely that circadian phosphorylation of these

proteins regulates the circadian rhythms of P_{Bmal1} and P_{Per2} activities. However, it is impossible to completely rule out this possibility from the data obtained in this study because phosphorylation of only a small portion of these proteins, such as the nuclear-located CLOCK/BMAL1 heterodimer, which may be difficult to detect from total protein samples, possibly regulate circadian oscillation in P_{Bmal1} and P_{Per2} activities (Brenna and Albrecht., 2020; Yoshitane et al., 2009).

Since the components of the core loop were not genetically manipulated in our *Bmal1*-inducible cell line, it is possible to assume that the intact core loop causes the P_{Bmal1} activity to oscillate. However, this does not seem to be the case. According to the DOX concentration, the amplitude of the oscillations in the P_{Bmal1} and P_{Per2} activities were simultaneously restored (Figure 8). These results suggested that there is no hierarchical relationship between P_{Bmal1} and P_{Per2} activities and that DOX-induced BMAL1 significantly affects both of P_{Bmal1} and P_{Per2} activities. In wild-type U2OS cells, P_{Bmal1} and P_{Per2} activities oscillate in antiphase because night-activated RORE in P_{Bmal1} and morning-activated E-box in P_{Per2} are incorporated into the interlocked feedback loops of activators and repressors (Ueda et., 2005). In the U2OS-P_{Bmal1}::*Fluc*/Δ*Bmal1*/P_{TRE3Gs}::*Myc-Bmal1* strain-2 cells, the antiphase relationship of P_{Bmal1} and P_{Per2} activities were still recapitulated even though functional *Bmal1* is not driven by endogenous P_{Bmal1} containing RORE, which cannot be explained by the current mammalian TTFL model.

Many mathematical models of circadian systems were proposed in the previous two decades (Asgari-Targi and Klerman., 2019). In these models, the behaviors of the mammalian TTFL components were expressed using a system of differential equations with experimentally determined parameters, including the activation and repression of clock genes transcription by clock gene products. In the model proposed by Mirsky et al., the constitutive expression of *Bmal1* is described by setting a constant value for the rate of *Bmal1* mRNA synthesis (Mirsky

et al., 2009). This model predicted that the levels of transcriptional and translational products of clock genes such as *Cry, Clock, Ror*c, *Rev-erb*α, as well as the translational product of *Bmal1* exhibit clear circadian oscillation even under constant levels of *Bmal1* mRNA. In contrast, the current study revealed no discernible rhythmicity in the levels of the BMAL1, CLOCK, and REV-ERBα proteins when *Bmal1* was expressed constitutively. For *Bmal1* transcriptional oscillations to be in the appropriate phase with respect to other clock genes, the high amplitude of oscillations in REV-ERB and ROR levels and their almost antiphase relationship are necessary (Relógio et al., 2011). Nevertheless, with the constant levels of REV-ERBα protein, our results demonstrate that P_{Bmal1} activity oscillated in the appropriate phase relationship relative to P_{Per2} activity. As a result, understanding these results using the mathematical models mentioned above is difficult.

It has long been accepted that the basis of the circadian clock is non-linear limit cycle oscillations in the field of chronobiology (Gonze and Ruoff, 2021). In this study, I found that the P_{Bma1} activity data were well-approximated by a second-order system that represents a linear damped oscillator in the presence of DOX at 1 μg/mL, and a third-order system that can be interpreted as a linear damped oscillator forced through a first-order system in the presence of DOX at 0.1 and 0.05 μg/mL. This finding can be a trigger to solving the oscillatory mechanism of the circadian clock because a linear system is much easier to analyze than a nonlinear one.

The damping coefficient (ζ) describes how quickly the oscillation decays. When the ζ is equal to 0, the oscillation continues stably without damping; when the ζ is between 0 and 1, the oscillation is damped, and when the ζ is higher than 1, no oscillation is observed. In all three conditions (DOX 1, 0.1, and 0.05 μg/mL) of oscillation, the ζ was quite small (Table 5), indicating that the damping of the oscillation was rather weak. The oscillation periods (τ) were all in a similar range between 24.8 and 25.6 h (Table 5). These results indicate that the

concentration of BMAL1 did not affect the oscillatory parameters (ζ and ω_n) significantly, but the baseline activity of P_{Bmal1} activity, shown by the first order component (Figure 15). It is possible that a weakly damped linear oscillator system, whose molecular mechanism is still unclear but is essentially independent of *BMAL1*, underlying the circadian clock and this oscillator regulates P_{Bma1} and P_{Per2} activities in parallel.

Based on the results of this study, I found that constitutively expressed *Bmal1* can restore rhythmicity in P_{Bmal1} activity. Expression levels of exogenous *Bmal1* affect the baseline but the period of circadian rhythms in P_{Bmal1} and P_{Per2} activities. At least in our experimental system, the roles of *Bmal1* in circadian oscillations seem to be different from those assumed in the current mammalian TTFL model. Further studies are required to determine whether the function of *Bmal1* described in this study is specific to our experimental system or is true for the mammalian circadian system.

References

Alessandro MD, Beesley S, Kim K, Chen R, Abich E, Cheng W, Yi P, Takahashi JS, and Lee C. A tunable artificial circadian clock in clock-defective mice. Nature Communication. 2015; 6:8587.

Asgari-Targhi A, and Klerman EB. Mathematical modeling of circadian rhythms. Wiley Interdisciplinary Reviews. System Biology Medicine. 2019; 11: e1439.

Balsalobre A, Brown SA, Marcacci L, Tronche F, Kellendonk C, Reichardt HM, Schütz, and Schibler U. Resetting of Circadian Time in Peripheral Tissues by Glucocorticoid Signaling. Science. 2000; 289: 2344 – 2347.

Beta RAA, Arsenopoulou ZV, Kanoura A, Dalkidis D, Avraamidou R, and Balatsos NAA. Core clock regulators in dexamethasone-treated HEK 293T cells at 4 h intervals. BMC Research Notes. 2022; 15(23).

Bozek K, Relo´ gio A, Kielbasa SM, Heine M, Dame C, Kramer A, and Herzel H. Regulation of Clock-Controlled Genes in Mammals. PLoS ONE. 2009; 4(3).

Brenna A and Albrecht U. Phosphorylation and Circadian Molecular Timing. Frontiers in Physiology. 2020; 11:612510.

Brown SA. Circadian rhythms. A new histone code for clocks?. Science. 2011; 333: 1833 – 1834.

Buhr ED and Takahashi JS. Molecular components of the mammalian circadian clock. Handbook of experimental pharmacology. 2013; 217: 3 – 27.

Cho H, Zhao X, Hatori M, Yu RT, Barish GD, Lam MT, Chong L, DiTacchio L, Atkins AR, Glass CK, Liddle C, Auwerx J, Downes M, Panda S, and Evans RM. Regulation of circadian behaviour and metabolism by REV-ERB-α and REV-ERB-β. Nature. 2012; 485:123 – 127.

Fagiani F, Marino DD, Romagnoli A, Travelli C, Voltan D, Mannelli L, Racchi M, Govoni S, and Lanni C. Molecular regulations of circadian rhythm and implications for physiology and diseases. Signal Transduction and Targeted Therapy. 2022; 7(41).

Fan Y, Hida A, Anderson DA, Izumo M, and Johnson CH. Cycling of cryptochrome proteins is not necessary for circadian-clock function in mammalian fibroblasts. Current Biology. 2007; 17:1091 – 1100.

Geo A and Kannan NN. Post-transcriptional modulators and mediators of the circadian clock. Chronobiology International. 2021; 38(9): 1244 – 1261.

Golnaraghi MF and Kuo BC. Automatic Control Systems. Volume 9. Prentice-Hall. 2009

Gonze D and Ruoff P. The Goodwin Oscillator and its Legacy. Acta Biotheoretica. 2021; 69(4): 857 – 874.

Griffin EA JR, Staknis D, and Weitz CJ. Light-Independent Role of CRY1 and CRY2 in the Mammalian Circadian Clock. Science. 1999; 286(5440): 768 – 771.

Guillaumond F, Dardente H, Giguere V, and Cermakian N. Differential control of Bmal1 circadian transcription by REV-ERB and ROR nuclear receptors. Journal of Biological Rhythms. 2005; 20: 391 – 403.

Haque SN, Booreddy SR, and Welsh DK. Effects of BMAL1 Manipulation on the Brain's Master Circadian Clock and Behavior. Yale Journal of Biology and Medicine. 2019; 92(2): 251 – 258.

Hughes ME, Hogenesch JB, and Kornacker K. JTK_CYCLE: an efficient nonparametric algorithm for detecting rhythmic components in genome-scale data sets. Journal of Biological Rhythms. 2010; 25: 372 – 380.

Kiyohara YB, Tagao S, Tamanini F, Morita A, Sugisawa Y, Yasuda M, Yamanaka I, Ueda HR, Horst GTJ, Kondo T, and Yagita K. The BMAL1 C terminus regulates the circadian transcription feedback loop. PNAS. 2006; 103(26): 10074 – 10079.

Ko CH and Takahashi JS. Molecular components of the mammalian circadian clock. Human Molecular Genetics. 2006; 15(2): 271 – 277.

Kojima S, Shingle DL, and Green CB. Post-transcriptional control of circadian rhythms. Journal of Cell Science. 2011; 124: 311 – 320.

Kume K, Zylka MJ, Sriram S, Shearman LP, Weaver DR, Jin X, Maywood ES, Hastings MH, and Reppert SM. mCRY1 and mCRY2 are essential components of the negative limb of the circadian clock feedback loop. Cell. 1999; 98: 193 – 205.

Lee C, Etchegaray PJ, Cagampang FR, Loudon AS, and Reppert SM. Posttranslational mechanisms regulate the mammalian circadian clock. Cell. 2001; 107: 855 – 867.

Lee CR, Park YH, Min H, Kim YR and Seok YJ. Determination of protein phosphorylation by polyacrylamide gel electrophoresis. Journal of Microbiology. 2019; 57: 93 – 100.

Liu AC, Tran HG, Zhang EE, Priest AA, Welsh DK, and Kay SA. Redundant Function of REV-ERBα and β and Non-Essential Role for Bmal1 Cycling in Transcriptional Regulation of Intracellular Circadian Rhythms. PLoS Genetics. 2008; 4(2).

Lück S, Thurley K, Thaben PF, and Westermark PO. Rhythmic Degradation Explains and Unifies Circadian Transcriptome and Proteome Data. Cell Reports. 2014; 9(2): 741 – 751.

Marghitu DB, Raju PK, and Mazilu D. Theory of Vibration. Mechanical Engineer's Handbook. 2001; 339 – 444.

Mirsky HP, Liu AC, Welsh DK, Kay SA, and Doyle FJ. A model of the cell-autonomous mammalian circadian clock. PNAS. 2009; 106: 11107 – 11112.

Ogata K. Modern Control. Engineering. Volume 5. Prentice-Hall. 2010.

Okamoto-Uchida Y, Izawa J, Nishimura A, Hattori A, Suzuki N, and Hirayama J. Post-translational Modifications are Required for Circadian Clock Regulation in Vertebrates. Current Genomics. 2019; 20(5): 332 – 339.

Ono D, Honma S, and Honma K.-i. Differential roles of AVP and VIP signaling in the postnatal changes of neural networks for coherent circadian rhythms in the SCN. Science. Advances. 2016; 2(9).

Oshima T, Yamanaka I, Kumar A, Yamaguchi J, Ohkawa T, Muto K, Kawamura R, Hirota T, Yagita K, Irle S, Kay SA, Yoshimura T, Itami K. C-H activation generates period-shortening molecules that target cryptochrome in the mammalian circadian clock. Angewandte Chem International Edition. 2015; 54: 7193 – 7197.

Pfaffl MW. A new mathematical model for relative quantification in real-time RT-PCR. Nucleic Acids Research. 2001; 29(9).

Preitner N, Damiola F, Molina, Zakany J, Duboule D, Albrecht U, and Schibler U. The orphan nuclear receptor REV-ERBα controls circadian transcription within the positive limb of the mammalian circadian oscillator. Cell. 2002; 110: 251 – 260.

Relógio A, Westermark PO, Wallach T, Schellenberg K, Kramer A, and Herzel H. Tuning the mammalian circadian clock: robust synergy of two loops. PLoS Compututational Biology. 2011; 7: e1002309.

Reppert SM and Weaver DR. Coordination of circadian timing in mammals. Nature. 2002; 418: 935 – 941.

Rijio FF and Takahashi JS. Genomics of circadian rhythms in health and disease. Genome Medicine. 2019; 11:82.

Ripperger, JA, Shearman LP, Reppert SM, and Schibler U. CLOCK, an essential pacemaker component, controls expression of the circadian transcription factor DBP. Genes and Development. 2000; 14: 679 – 689.

Robles MS, Humphrey SJ, and Mann M. Phosphorylation is a central mechanism for circadian control of metabolism and physiology. Cell Metabolism. 2017; 25: 118 – 127.

Sato TK. Panda S, Miraglia LJ, Reyes TM, Rudic RD, Namara PM, Naik KA, FitzGerald GA, Kay GS, and Hogenesch JB. A functional genomics strategy reveals Rorα as a component of the mammalian circadian clock. Neuron. 2004; 43: 527 – 537.

Serin Y and Acar Tek N. Effect of Circadian Rhythm on Metabolic Processes and the Regulation of Energy Balance. Annals of Nutrition and Metabolism. 2019; 74: 322 – 330.

Takahashi JS. Transcriptional architecture of the mammalian circadian clock. Nature Reviews Genetics. 2017; 18(3):164 – 179.

Tamaru T, Hirayama J, Isomija Y, Nagai K, Norioka S, Takamatsu K, and Sassone P. CK2alpha phosphorylates BMAL1 to regulate the mammalian clock. Nature Structural and Molecular Biology. 2009; 16: 446 – 448.

Ueda HR, Hayashi S, Chen W, Sano M, Machida M, Shigeyoshi Y, Iino M, and Hashimoto S. System-level identification of transcriptional circuits underlying mammalian circadian clocks. Nature Genetics. 2005; 37: 187 – 192.

Yoshitane H, Takao T, Satomi Y, Du N, Okano T, and Fukuda Y. Roles of CLOCK phosphorylation in suppression of E-box-dependent transcription. Molecular and Cellular Biology. 2009; 29: 3675 – 3686.